OPTIMIZATION OF SURFACE PROPERTIES OF ACTIVATED CARBON FROM PERIWINKLE SHELL USING RESPONSE SURFACE METHODOLOGY

BY

(UCHENNA UGOCHUKWU EKESIOBI)

(MAT NO: ENG/1818504)

DEPARTMENT OF CHEMICAL ENGINEERING,

FACULTY OF ENGINEERING,

UNIVERSITY OF BENIN

BENIN CITY.

A PROJECT SUBMITTED TO THE DEPARTMENT OF CHEMICAL ENGINEERING

IN PARTIAL FULFILMENT OF THE REQUIREMENT FOR THE AWARD OF THE DEGREE OF

MASTERS OF ENGINEERING (M.ENG) OF CHEMICAL ENGINEERING

DECEMBER, 2021

CERTIFICATION

This is to certify that this research project submitted to the Department of Chemical Engineering was carried out by UCHENNA UGOCHUKWU EKESIOBI, of the Department of Chemical Engineering, Faculty of Engineering, University Of Benin, Benin City, Edo State, Nigeria.

....

ENGR. DR. (MRS.) E.A.OYEDOH **Date**

PROJECT SUPERVISOR

....

ENGR. DR. (MRS.) E.A.OYEDOH **Date**

HEAD OF DEPARTMENT

....

MR . N.A. IHOEGHIAN **Date**

PROJECT CORDINATOR

....

External Examiner **Date**

DEDICATION

This research project is dedicated first to “THE ALMIGHTY GOD” for his enabling strength and provisions he bestowed on me in completing this work. Secondly to my lovely wife Mrs. Sandra Uchenna-Ekesiobi, my mother Mrs Victoria Ekesiobi, and my late father, Late Mr Ignatius Ekesiobi.

ACKNOWLEDGEMENTS

I am most grateful to God Almighty, the sole provider of knowledge, wisdom, love, mercy and grace for his provisions and protections throughout the period of the programme. I sincerely appreciate my supervisor, **ENGR. DR. (MRS.) E.A.OYEDOH** for her motherly advice, support and corrections that led me through the various stages of this project.

I appreciate my wife, Mrs. Sandra Uchenna-Ekesiobi, my children, my siblings and friends for their unquantifiable love and financial assistance during this period. May God bless you all in Jesus name, Amen.

I appreciate my course mates, Mr Akpali Emmanuel, Rapheal, Osaigie, Kpante Kenneth and Ogaga for their unquantifiable support and academic assistance during this period. May God bless you all in Jesus name, Amen.

ABSTRACT

The relative utilization of activated carbon has constantly increased with the advancement in modern technology. In a bid to make use of alternative precursors for activated carbon production, periwinkle shells were used.

This study explored the use of periwinkle shells for the production of periwinkle shell activated carbon (PSAC) prepared using potassium hydroxide (KOH) activation method. The adsorbent was characterized using the Fourier Transformed Infrared (FTIR) analysis. Central composite design (CCD) in response surface methodology (RSM) was used for the optimization of PSAC production conditions. Quadratic models and linear model were developed for the percentage yield of PSAC, the surface area and the porosity. Model suitability was validated using Analysis of Variance (ANOVA). The FTIR analysis showed the presence of stretching vibration bands such as carbonate ion (CO_3^{-2}), aliphatic N-H and heterocyclic N-H. The optimum conditions for PSAC production was 536.375^{o}C and 82.087minutes for activation temperature and activation time respectively. This led to maximized responses; PSAC's yield percentage of 95.147%, surface area of 71.525m^2/g and porosity of 36.695. The correlation coefficient R^2 obtained were very high for each response; 99.47%, 99.98% and 97.77% for PSAC's yield, surface area and porosity respectively indicating that the results of experimental studies were in perfect agreement with those suggested from model. Thus, the prediction by the model was in good conformity with actual results. Periwinkle shells were found to attain PSAC that had a very high yield as well as excellent surface area and porosity.

TABLE OF CONTENTS

LIST OF FIGURES

LIST OF TABLES

CHAPTER ONE

INTRODUCTION

1.1 BACKGROUND OF STUDY

In 2017, the global activated carbon (AC) market was worth $4.12 billion, and by 2026, it is predicted to be worth $14.21 billion (S. M. R. C. P. Ltd, 2018). An increasing demand for water treatment plants, rising pollution, and greater industry and urbanization are all key growth factors. The high cost of raw materials, on the other hand, limits the product's rapid expansion (Ahmad et al., 2020).

The relative utilization of activated carbon has constantly increased with the advancement in modern technology. On this basis, innovators are seeking to find the different ways it can be obtained and harnessed. In recent times, the production of activated carbon from biomass, especially agricultural wastes, has gained enormous interest. Activated carbon was initially gotten from petroleum or coal. Recently, it is now being produced from wood, waste cocoa pod walnut shells, groundnut shells, coconut shells, snail shells, periwinkle shells.

Activated carbon is a type of carbon that possess outstanding physicochemical qualities that allow it to be utilized in a wide range of applications. ‘Activated carbon has a variety of applications, including catalysis, gas purification, chemical storage and purification, and electrode material for energy storage systems. The properties exhibited by activated carbon include high surface area, variable pore size and volume, chemical inertness and stability (Abioye & Ani, 2015; Banerjee et al., 2020)’. The majority

of commercial activated carbons are made from fossil fuel-based precursors (petroleum and coal), thus making them expensive and environmentally unfriendly. As a result, more emphasis is being placed on biomass precursors, which are less expensive, more readily available, renewable, structurally porous, and environmentally friendly(Abbas & Ahmed, 2016; Abioye & Ani, 2015; Farma et al., 2013).

Periwinkles are marine snails that belong to the shellfish family Gastropod mollusc. They can be found in oceans all over the world. In Nigeria, the *T. fuscautus* species is the most abundant and it is commonly found in the Niger-Delta region. Periwinkles can be found in a variety of locations along the shore. Its height ranges from half an inch to one inch, and its colour ranges from grey to black. The shell is substantial and heavy (Badmus and Audu, 2009).

Periwinkle shell is the by-product obtained after the edible part of the periwinkle shellfish is removed. Winkles, abalones, and conchs represent around 2.8% of the 16 million tonnes of mollusc shellfishes globally produced each year through aquaculture (Eziefula et al., 2020), FAO, 2016). The shell of a mollusc shellfish accounts for about 70% of its weight depending on the species; considering that the shell is not edible, a large fraction of shellfish production is considered as waste. Periwinkle shell wastes are commonly piled in open fields and landfills, resulting in a foul odor, ugly appearance, and the development of disease-carrying organisms(Morris et al., 2019). In order to mitigate the environmental impact of the shells several alternative uses have being developed over time. One of which is the production of activated carbon from periwinkle shells. Periwinkle shells provide a very cheap, sustainable and rich source of carbon. Also, compared to commercial activated carbon (CAC), the production process for

periwinkle shell activated carbon (PSAC) is more eco-friendly(Banerjee et al., 2020; Wang et al., 2017).

The properties of the activated carbon produced is dependent on number of factors.(Banerjee et al., 2020) stated that factors such as; the type of biomass precursor used, activation temperature, activation time, impregnation rate, the type of functional group, content of heterofoam, extent of graphitization have a way of affecting the properties of the activated carbon. In order to produce activated carbon with the best surface properties, these factors have to be optimized. Activated carbon synthesis using the “one factor at a time” method does not show the interaction between factors (A. A. Ahmad et al., 2020) thus the need for optimization.

1.2 PROBLEM STATEMENT

Waste disposal has remained the predominant source of environmental and soil pollution in the world, especially in Nigeria. Although agricultural wastes eventually decompose, it does so slowly and leaves the environment unsightly for a long period of time. Having a medium to convert these wastes to either source of renewable energy or raw materials would not only make the environment cleaner, it would also help to eliminate the cost of waste disposal.

The traditional means of obtaining commercial activated carbon (CAC) is very expensive and non-environmentally friendly. The energy requirement for this process (above 1000^{o}C for pyrolysis) (Faraji & Ani, 2015), makes it economically unattractive.

The demand for activated carbon continues to grow. As more academics uncover new applications for activated carbon, the number of sectors that use it tends to increase. It

is necessary to not only generate activated carbon from a low-cost source, but also to produce activated carbon with excellent surface properties with the ability to suit the specified needs. The inability of the traditional experimental method of changing “one-factor-at-a-time” to determine the effect of the interactions between factors affecting the process output. (comment; paraphrase)

The utilization of periwinkle shell for the production of activated carbon would;

- Mitigate environmental pollution resulting from shell piles. This would also minimize the expenditure on waste disposal.
- Provide a more economically attractive and eco-friendly means to produce activated carbon to satisfy its need in various industries.

By optimizing the production process, lesser time is spent producing and more experiments can be conducted thus making the process more economical and feasible.

1.3 AIMS AND OBJECTIVES OF STUDY

The aim of this research work is to optimize the surface properties of activated carbon produced from periwinkle shells using Response Surface Methodology (R.S.M). To achieve this aim the following objectives will be pursed;

1. Production of activated carbon from periwinkle shell
2. Investigate the effect of activation temperature and time on the yield, porosity and surface area of activated carbon.
3. Optimization of surface properties using Response Surface Methodology

1.4 SIGNIFICANCE OF STUDY

Activated carbon has the strongest physical adsorption forces or the highest volume of adsorbing porosity of any material known to mankind, its usefulness cannot be overemphasized in the treatment of water and effluent generated in industries amongst other uses. This has increased the demand for activated carbon over time. This study/research will provide the necessary experimental data to harness the commercial production of the activated carbon from periwinkle shell at an optimal cost. This research would also play a vital role of mitigating environmental pollution caused by the disposal of periwinkle shells. Overall, this study if harnessed and scaled up would have a positive impact on the economics of the country.

1.5 SCOPE OF STUDY

This study is limited to:

- Collection and preparation of the raw material.
- Production of activated carbon from periwinkle shells.
- Determination of the surface properties of the activated carbon.
- Use of Design of Experiment to study the parameters.
- Optimization using Response Surface Methodology (RSM)
- FTIR analysis.

CHAPTER TWO

LITERATURE REVIEW

2.1 ACTIVATED CARBON

Activated carbon, often known as activated charcoal, is a crude form of graphite with an amorphous nature. It has a random, flawed microstructure that is very porous over a wide range of pore sizes, from apparent cracks and crevices to molecular dimensions. The carbon's high surface area is due to its amorphous structure, which allows it to adsorb a wide spectrum of chemicals

Figure 2.1: Activated Carbon granules
Source @ https://alumichem.com/our-products/chemistry/activated-carbon/

Activated carbon has the strongest physical adsorption forces of any substance known to mankind, as well as the largest volume of adsorbing porosity. The surface area of activated carbon can be larger than 1000m^2/g. This equates to 5g of activated carbon can have the surface area of a football field(Arvanitoyannis et al., 2008).

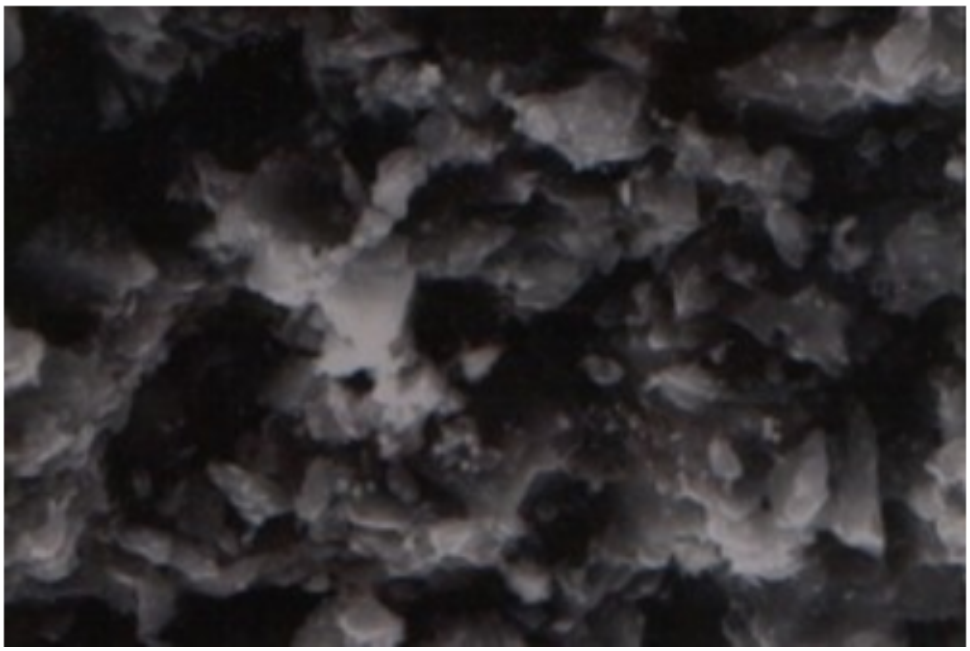

Figure 2.2: Microscopic View of Activated Carbon
Source @ https://www.desotec.com/en/carbonology/carbonology-academy/chemical-structure-activated-carbon

2.1.1 HISTORY OF ACTIVATED CARBON

The precise date and period when man first started using activated carbon or charcoal has been lost to history. However, evidence of its use and significance can be found throughout history, from the ancient world to the contemporary era.

Charcoal was used by the Ancient Egyptians to process ores into bronze around 3750 B.C. The Egyptians' usage of charcoal had developed by 1500 B.C., according to the first documented use of charcoal on papyrus, with the material being used to absorb bad odors, alleviate intestinal diseases, and even preserve the dead. Charcoal was first used to filter water by the Ancient Hindus and Phoenicians in 400 B.C. due to its antibacterial characteristics. On long sea trips, the Phoenicians were known to char barrels to keep water. Many other mariners, including Christopher Columbus, embraced this practice

throughout history and practiced it until the 1800s. Hippocrates, one of the most famous characters in medical history, began employing charcoal for a variety of medical uses around 50 A.D., including treating epilepsy, chlorosis, and vertigo. Claudius Galen, another prominent person in medical history, wrote around 500 treatises on the use of charcoal in medicine by the year 2 A.D.

Though charcoal has been in use for millennia, it saw a dramatic rebirth in the late 1700s. More doctors, chemists, and other scientists began testing the material for medical and manufacturing applications. Carl Wilhelm Scheele, a chemist, measured the volume of gases adsorbed by porous carbon in 1773 and calculated the adsorption forces. Lowitz, recognizing the adsorptive qualities of charcoal in liquid phase, performed the first experiments that established that carbon could be used to decolour solutions in 1776.

However, in 1794, an English sugar refinery discovered that carbon could be employed as a decolouring agent, making it one of the most significant discoveries of the period. The sugar business, which had been looking for a solution to make a whiter, more appealing product, was completely transformed as a result of this. As a result of this advancement, activated carbon research has progressed even farther. By 1805, all of Europe had adopted charcoal as a method of sugar decolourization.

In the nineteenth century, charcoal remained a powerful force, particularly in medicine. Poultices, sloughing ulcers, and treating gangrenous sores were all common uses. Around 1820, the activated carbon method was first described in medical journals as a poison antidote and a treatment for digestive ailments. Gabriel Bertrand, a French

chemist, drank arsenic mixed with charcoal in an attempt to illustrate charcoal's worth as a poison remedy in 1883. Others imitated him and pulled off the same stunt. Frederick Lipscombe used activated carbon to purify drinkable water in 1862, paving the way for commercial applications of the material. Heinrich Kayser, a German physicist, created the term "adsorption" to characterize charcoal's propensity to absorb gases. Activated carbon was initially manufactured on a large scale in the early twentieth century. In 1909, the "Chemische Werke" was created to manufacture carbon for commercial usage, creating Eponit, Purit, Norit, and Calgon, among other carbons. The Norit Company, a Dutch business, was founded in 1911 and quickly gained a reputation in the sugar industry for its powdered solutions, which are widely used in the chemical and food industries. During World War I activated carbon was used in gas masks worn by American soldiers to protect them from poison gas. This development led to the production of granular carbon on a large scale.

The utilization of activated carbon is expanding today. It is utilized on a regular basis in almost every hospital, clinic, and doctor's office around the world. Corn and cane sugar refining, gas adsorption, dry cleaning, medicines, fat and oil removal, alcoholic beverage production, and other sectors use the substance. The treatment of municipal water sources is the major market for activated carbon. When water is disinfected, activated carbon filters are employed to eliminate organic chemicals that produce carcinogens. The removal of heavy metals from coal fire powder is the second largest market for activated carbon.

2.1.2 STRUCTURE OF ACTIVATED CARBON

POROUS STRUCTURE OF ACTIVATED CARBON

The porous properties of activated carbon, such as pore volume, pore size distribution, porosity and surface area, determine its increased adsorption capability. Up to 15% of ash in the form of mineral matter can be found in activated carbon (Bansal et al 1988). Activated carbon develops a porous structure during the carbonization process and continues to develop during activation. The porous structure of activated carbons is present in all of them. The pore system of activated carbon is divided into several categories, with each pore varying in size and shape. Pore sizes in activated carbons range from a few nanometers to thousands of nanometers. Pores are categorized according to their average width. The average width of a pore is the distance between its walls, or the radius of a cylindrical pore. (Dubinin et al 1960) developed conventional categorization, which was formally adopted by the International Union of Pure and Applied Chemistry (IUPAC). A typical pore size classification is shown below in table 2.1

Table 2.1: Classification of Pore Sizes

Type of Pore	Width
Micro pore	<2.0nm
Meso pore	2.0 – 50.0nm
Macro pore	>50.0nm

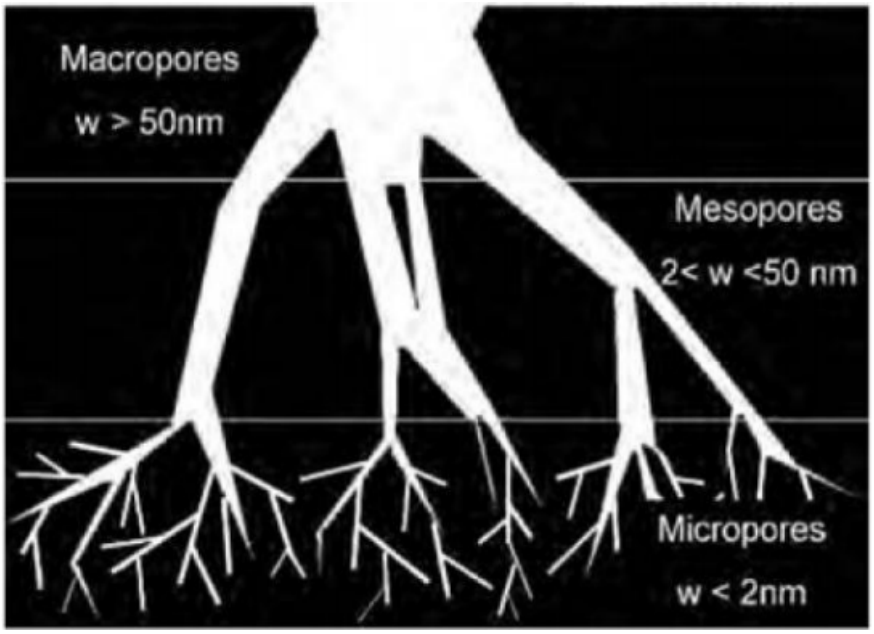

Figure 2.3: graphical representation of pore structure of activated carbon

CRYSTALLINE STRUCTURE

Activated carbon develops a microcrystalline structure during carbonization. In terms of interlayer spacing, the structure of activated carbon differs from that of graphite. Interlayer spacing in graphite is 0.335 nm, while it is 0.34 to 0.35 nm in activated carbon. Activated carbons are divided into two categories based on their graphitizing ability: graphitizing and non-graphitizing. There are a number of graphene layers positioned parallel to each other in graphitizing carbon. Because of the weak cross connecting between neighboring micro crystallites, the carbon produced was fragile and had a less developed porous structure. Non-graphitizing carbons are hard due to strong cross linking between crystalline structure and a well-developed micro pore structure (Franklin 1951, Jenkins and kawamura 1976). The presence of related oxygen or a deficiency of hydrogen in the initial raw material promotes the creation of non-graphitizing structures

with strong crosslinks. Figure 2.4 illustrates schematic representations of the structures of graphitizing and non-graphitizing carbons.

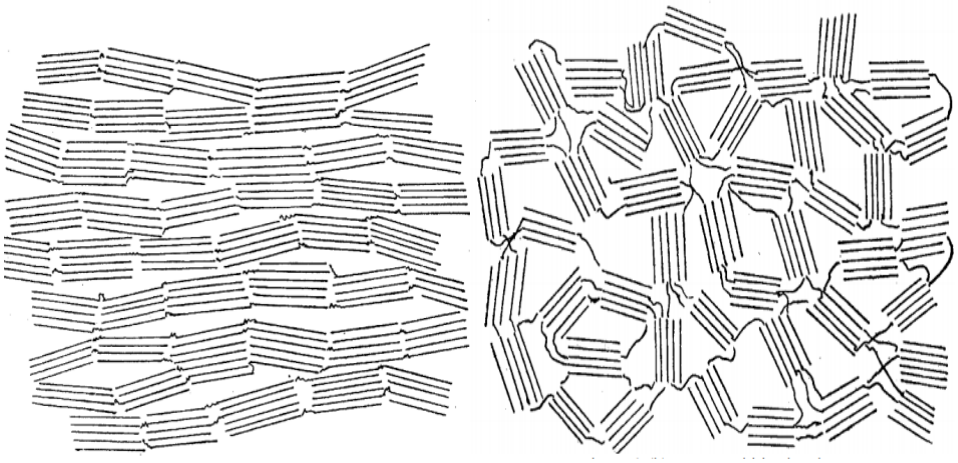

Figure 2.4 (a) graphitizing carbon (b) non-graphitizing carbon

CHEMICAL STRUCTURE

Activated carbon has both a porous and crystalline structure, as well as a chemical structure. Though the porous structure of activated carbon determines its adsorption capacity, it is substantially impacted by a relatively modest number of chemically bound functional group (mostly oxygen and hydrogen) (Bansal et al., 1988). The organization of electron clouds in the carbon skeleton varies, resulting in the formation of unpaired electrons and incompletely saturated valences, which alters the adsorption capabilities of active carbons, particularly for polar molecules.

2.1.3 PROPERTIES OF ACTIVATED CARBON

Each variation of each base calcined structure has its own unique, predictable

properties. This allows one to select the form of activated carbon that best suits a specific application. They include;

Pore Size: Activated carbon eliminates undesirable substances by the adsorption process, in which the targeted material binds with carbon atoms along the surface of the activated carbon. The activation process forms a large submicroscopic porosity network, which greatly increases the number of bonding sites available. Varied applications, however, necessitate different pore diameters. Micro porous activated carbon has pores smaller than 2 nanometers. The pore size of "mesoporous" activated carbon is 2 to 5 nm, while "macro porous" activated carbon has a pore size more than 5 nm.

Iodine numbers: The iodine number is the most fundamental parameter used to characterize activated carbon performance. Iodine number (generally 500 to 1200 mg/g) measures the adsorption capability for small molecules. It is defined as the milligrams of iodine adsorbed by 1.0 g of carbon when the iodine concentration of the filtrate is 0.02 N (0.02 mol/L) (Nunes & Guerreiro, 2011). The iodine capacity, mg/g, (ASTM D28 Standard Method test) may be used as an indication of total surface area. It is a measure of the micropore content of the activated carbon (0 to 20 Å, or up to 2.0nm) by adsorption of iodine from solution. It is equivalent to surface area of carbon between 900 and 1100 m^2/g. It is the standard measure for liquid-phase applications (Mianowski et al., 2007).

Molasses Numbers: The molasses number (typically 95 to 600 mg/g) shows the capability to adsorb large molecules. Molasses number or molasses efficiency is a

measure of the mesopore content of the activated carbon (greater than 20 Å, or larger than 2 nm) by adsorption of molasses from solution. Molasses Number is a measure of the degree of decolorization of a standard molasses solution that has been diluted and standardized against standardized activated carbon. Due to the size of color bodies, the molasses number represents the potential pore volume available for larger adsorbing species. Because all of the pore volume may not be available for adsorption in a particular waste water application, and as some of the adsorbate may enter smaller pores, it is not a good measure of the worth of a particular activated carbon for a specific application. This parameter is useful in evaluating a series of active carbons for their rates of adsorption. Given two active carbons with similar pore volumes for adsorption, the one having the higher molasses number will usually have larger feeder pores resulting in more efficient transfer of adsorbate into the adsorption space.

Methylene blue Number: The methylene blue number (often 11 to 28 g/100g) indicates the adsorption capability for medium-sized molecules. It is defined as the maximum amount of dye adsorbed on 1.0 g of adsorbent (Nunes & Guerreiro, 2011).

Tannin Numbers: Since most contaminants contain a variety of molecule sizes, the tannin number (normally 200 to 362 ppm) demonstrates the capability of the activated carbon to adsorb mixtures.

Carbon tetrachloride activity (CTC): This is the porosity of activated carbon for air/vapor applications, and it ranges from 45 to 70% by weight.

Dechlorination: This is the depth an activated carbon bed must be to remove half the chlorine from a liquid stream (known as the half-value). The lower the half-value of an

activated carbon bed, the better its performance.

2.1.4 FORMS OF ACTIVATED CARBON

It is difficult to classify activated carbon based on their behavior or surface properties. However on the basis of the physical characteristics such as size, activated carbon can be classified mainly into three (3), namely; *Granular activated carbon, powdered activated carbon* and *extruded activated carbon.*

Granular Activated Carbon (GAC):

It has a substantial particle size ranging from 0.2 to 5mm and, as a result, has a smaller exterior surface area. This type of activated carbon is utilized in both liquid and gas phase applications. They are utilized in flow systems and quick mix basins for air filtration and water treatment, as well as general deodorization and component separation.

Powdered Activated Carbon (PAC):

According to ASTM classification, it is termed finer or pulverized carbon with a size generally less than 0.18mm (US Mesh 80). These are mostly employed in liquid phase applications and in the treatment of flue gases. Because of the considerable head loss that would occur, it is uncommon to use PAC in a specialized vessel. Instead, PAC is commonly fed to various process units such as raw water intakes, fast mix basins, clarifiers, and gravity filters directly.

Extruded Activated Carbon (EAC):

This type of activated carbon is created when powdered activated carbon and a binder is fused together and extruded into a cylinder shaped activated carbon block with

diameters ranging from 0.8 to 130 mm. Due to their minimal pressure drop, strong mechanical strength, and low dust content, these are mostly used in gas phase applications. (Kyotani, 2003)

2.1.5 APPLICATION OF ACTIVATED CARBON

Activated carbon is applicable in diverse fields. It finds its usefulness in water treatment, chemical and petroleum industries, separation, purification, catalysis, energy storage, batteries, fuel cells, nuclear power stations, electrodes for electric double layer capacitors, pharmaceutical, hydrometallurgy and others.

- Activated carbon can be used in the food industry for decolourization, deodorization, and flavor removal.
- It is utilized in medicine for the adsorption of hazardous chemicals and drugs.
- Activated carbon is utilized in gas cleaning applications for air filters and air conditioning.
- Activated carbon has been used in the mineral sector to recover gold from leached liquors, for example.

2.2 PRODUCTION OF ACTIVATED CARBON

The production of activated carbon is usually a two-stage process; ***carbonization*** and ***activation*** (Kwiatkowski, 2008). Biomass, coal, petroleum, forestry waste, and agricultural residues are utilized as raw materials in the production of activated carbon. For the production of activated carbon, the precursor employed must be high in carbon

content. The necessity of obtaining the most homogenous porous structure dictates the use of the two stages in the active carbons production process. Both of these processes, however, have a major impact on the characteristics of the porous structure that develops. As a result, optimizing the manufacturing process parameters and selecting the best method and reagents is one of the most important issues in the production of active carbons(Kwiatkowski, 2008).

2.2.1 CARBONIZATION PROCESS

Carbonization, also known as pyrolysis, is the process of heating input raw materials to temperatures below 800°C without the presence of air or in a continuous stream of inert gas(Kwiatkowski, 2008). Most non-carbon elements, hydrogen, and oxygen are eliminated in gaseous form during the carbonization process by pyrolytic destruction of the raw materials, and the free atoms of carbon are clustered into elementary graphite crystal lattice (Kyotani, 2003). The carbonization process comprises the thermal breakdown of carbonaceous materials to remove non-carbon species, resulting in a semi-finished product termed carbonisate with an undeveloped pore structure.

In the course of the carbonization process, certain parameters greatly influence the process outcome. Such parameters include; temperature, heating rate, pressure, atmosphere, and properties of the raw material, such as its structure, elemental composition, humidity, the contents and composition of mineral matter, and the composition and size of grains(Kwiatkowski & Broniek, 2017). The carbonisate has a poorly developed porous structure and a low adsorptive capacity, rendering it ineffective in the majority of adsorption operations. The carbonization process includes several

critical phases that significantly influence the qualities of the final product. Around 500^{o} C, the basic microstructure of the char with microporosity is formed. Some of these pores are sealed by the tarry compounds formed during pyrolysis and may be accessible only after a subsequent heat treatment to around 800°C.Further heat treatment to 1000^{o}C and above usually results in hardness of the carbon structure due to partial alignment of graphitic planes and a decrease in porosity, both of which slow down activation. Consequently, the carbonisate is physically or chemically activated to obtain the necessary degree of porosity structure growth (Kyotani, 2003).

2.2.2 ACTIVATION PROCESS

Following the carbonization of the precursor for the production of activated carbon is the process of activation. The purpose of activation is to increase the diameters of the pores formed during the carbonisation process and to create new porosity, resulting in the production of a well-developed and easily accessible pore structure with a very large interior surface area. Activation is accomplished in two ways, as detailed in the following sections (Kyotani, 2003).

2.2.2.1 PHYSICAL ACTIVATION

It is a method in which the carbonized product develops a porous structure with molecular dimensions and a large surface area after being heated to temperatures ranging from 800 to 1000 degrees Celsius in the presence of suitable oxidizing gases such as steam, CO2, and air (ACS 1996). Activation temperature is the determinant of the course of reaction and the development of the porous structure, and as such it should be selected with due care. Seeing as low process temperatures may alter reaction kinetics due to the endothermic nature of the reaction, the temperature should

be quite high. At the right temperature, the activation process reactions occur on the inner surface of carbon, and carbon is taken from the pore walls as a result of the aforementioned processes, causing the pores to widen. However, extremely high temperatures may cause a reaction on the outer surface of carbon molecules. When oxygen or air is used as the activating agent, the reaction moves very quickly due to these agents' strong reactivity, and the carbonisate burns off in an unregulated way. Uncontrolled burn-off causes the formation of a porous structure and significant material losses, as well as the generation of vast volumes of surface oxides. As a result, in the vast majority of situations, oxygen and air are not advised as activation agents. Certain materials, even extremely little concentrations of particular chemicals, can greatly speed up the physical activation process. KOH and K2CO3 are utilized as physical catalyzers in industrial applications(Kwiatkowski, 2008; Kwiatkowski & Broniek, 2017).

Physical activation has several advantages, including a cheap cost of manufacture of activated carbons and the ability to keep the shape and texture of the raw material, allowing for the manufacturing of activated carbon fabrics and cloths, for example.

Physical activation, on the other hand, produces activated carbons with a specific surface area of less than 2000 m2/g. Furthermore, the bulk of the raw material is reduced by up to 70% during the process, and two distinct high-temperature carbonization procedures necessitate large energy expenditures.

2.2.2.2 CHEMICAL ACTIVATION

Chemical activation entails impregnating the raw material with a sufficient amount of an activating agent such as salts, alkali, metal hydroxides, carbonates, sulphates,

nitrates, as well as nitric, sulphuric and phosphorous acids, usually in the form of a concentrated solution, and then carbonizing it in a neutral atmosphere. To remove the remaining activating ingredient, the carbonisate is cooled and washed with distilled water or mild acid(Kwiatkowski & Broniek, 2017; Nunes & Guerreiro, 2011).

The type of raw material, process temperature, the atmosphere of the activation process, and impregnation ratio, i.e. the ratio of the activating agent to the raw material, all affect the formation of the porous structure during chemical activation. The impregnation ratio, i.e. the ratio of the activating agent to the raw material, has a particular impact on pore quality and pore size distribution. Higher impregnation ratios usually result in bigger pore capacity and surface area of the activated products.

Chemical activation procedures have a number of advantages over physical activation. Chemical activation, for example, minimizes the generation of tar during pyrolysis, enhancing the efficiency of the process. Chemical activation can also be done at lower temperatures and for shorter periods of time than physical activation, resulting in a more porous structure. As a result, less energy is needed throughout the method, resulting in cheaper production costs.

KOH has been discovered to be useful as an activating agent in the manufacture of activated carbon with a narrow pore size distribution and well-developed porosity. The activation process using alkaline metals such as KOH has been postulated, in which the alkali metal interlinks in the carbon lattice and acts as an electron donor, sparking the reaction during gasification. The presence of oxygen in the alkali could prevent the carbon atoms in the crystallites from cross-linking. Potassium metal liberation at high

temperatures interacts and forces a portion of the crystallite's distinct layers together. When compared to ZnCl2, the usage of KOH has been recommended to be more environmentally beneficial (Yahya et al., 2015).

Chemical activation also allows for more precise control of porosity formation. Chemical activation, on the other hand, has several disadvantages, such as the need for an additional rinse stage to remove excess activating agent, the chance that contaminants originating from the activating agent would stay in the created material, and additional chemical reagent expenditures.

In modern activated carbon production technologies, a combination of physical and chemical activation methods is increasingly being utilized.

2.3 PRECURSOR FOR ACTIVATED CARBON PRODUCTION

Coal and agricultural byproducts or lignocellulosic materials are the two main sources of activated carbon production. Precursors used in commercially activated carbon include petroleum wastes, wood, coal, peat, and lignite, all of which are very expensive and non-renewable. As a result, in recent years, people have been concentrating on activated carbon preparations based on agricultural waste and lignocelluloses materials that are both effective and inexpensive, such as corncob, hazelnut shell, pruning mulberry shoot, olive stone, Jojoba seed, Chinese fir sawdust, coconut shell, wood, hazelnut bagasse, kenaf fiber, bamboo, rice husk, petai, groundnut shell, and paper mill sludge (Yahya et al., 2015).When compared to anthracite, coal, or peat, these by-products have a lower carbon concentration. As a result, activated carbon yields from these precursors are projected to be reduced. Its lower cost, on the other hand, has a

greater impact than its lower yield. The high volatile matter concentration of biomass has proved excellent for producing a highly porous activated carbon structure. The usefulness of the waste's end products, particularly activated carbon, and the economic input that may be received from these valuable products can eventually offset treatment and disposal expenses.

2.3.1 PERIWINKLE SHELLS AS A PRECUSOR FOR ACTIVATED CARBON PRODUCTION

Periwinkles are marine snails that belong to a group of shellfishes known as gastropod mollusc. Among the several species of periwinkle shellfish include *Littorina littorea, Nodilittorina radiata, Tympanostomus fuscatus,* and *Pachmellania aurita*. Periwinkles inhabit the aquatic region between low and high tides. Although they live near the ocean and spend part of their time under water, periwinkles prefer to be partially exposed to air. Periwinkles are soft but are typically surrounded and protected by strong, brittle, and hard shells (Eziefula et al., 2020). They are found in oceans all over the world. The common periwinkle (*Littorina littorea*) is one of the most abundant marine gastropods on the North Atlantic but, T. *Fuscatus* is commonly found in the Niger-Delta, Nigeria. Periwinkles distribute themselves in different positions on the shore. It is approximately one-half inch to one inch in height, and is grey to black in colour. The shell is fairly heavy and solid. They live in the intertidal zone (the area of the shore that has alternating periods of exposure to air and then water) (Badmus & Audu, 2009). *T. fuscatus* is characterized by turreted, granular, and spiny shells with tapering ends as seen in figure 2.5.

Figure 2.5: Periwinkle shells of Typanotonus Fuscatus species
Source https://www.schooldrillers.com/african-periwinkles/

A periwinkle shell has spikes which makes it rough-textured. The maximum diameter of periwinkle shells varies from 10 to 20 mm at one end and tapers to a point at the other end; the length varies from 20 to 60 mm (Falade, 1995). The mineral phase of periwinkle shell is made of chitin and nacre, an organic mixture of outer layer of horny conchiolin which is a sclero protein, followed by an intermediate layer of calcite or aragonite polymorphs and also a layer of calcium carbonate (Ugoeze and Chukwu, 2015). Molluscan shells are basically comprised of about 95 to 99% $CaCO_3$ with a small amount of chlorides, sulfates, and organic substances (Olivia et al., 2015; Yao et al., 2014) Heat treatment of seashells helps to improve the shell quality through dehydration and disinfection as well as safe handling and storage(Eziefula et al., 2020; Yao et al., 2014). Heat treatment of seashells also has the prospect of yielding higher Carbon content (Eziefula et al., 2020)

2.4 FACTORS DECIDING THE PROPERTIES OF ACTIVATED CARBON

In order to prepare high performance activated carbon, it is important to maintain a suitable control over the following parameters during preparation stage.

Raw Materials: The precursor for the synthesis of activated carbon includes a variety of organic compounds with high carbon content. A variety of factors influence the formation of porous carbon structured activated carbon, including high carbon content, low inorganic or ash content, high density, sufficient volatile content, stability and minimal degradation during storage, and low cost.

Surface Area and Pore Size Distribution: The key criteria that determine the physicochemical features of activated carbon are temperature and the choice of activating agent. High temperatures cause carbonaceous species to decompose and increase crystallinity. Extreme crystallinity, on the other hand, reduces surface area.

Extent of Graphitization: High-temperature annealing promotes graphitization by causing the graphite lattice to self-heal, causing the carbon network around the heteroatom to decompose. Although graphitization increases the conductivity of the carbon matrix, it also causes the depletion of heteroatoms, lowering the carrier concentration.

Content of Functional Groups: The presence of surface functional groups promotes ion adsorption at the carbon matrix's surface. Over doping different functional groups, on the other hand, has a steric impact, reducing conductivity within the carbon network.

Surface Concentration of Functional Group: The presence of surface-active species increases the carbon matrix's surface properties. To achieve the required surface

properties of the carbon matrix, a sufficient number of surface functional groups are required.

Type of Functional Group: Along with the carbon matrix, functional groups functions either boost reactivity or increase conductivity. Pyridinic-N, for example, serves as a Lewis base, whereas graphitic-N enhances conductivity(Banerjee et al., 2020; Rana et al., 2017).

Activation Time: The carbonization process and the final properties of activated carbon are greatly influenced by the activation time. The activation period is directly proportional the BET () surface area and inversely proportional to the percentage yield of activated carbon. This could be due to the volatilization of organic compounds during the carbonization process.

Activation Temperature: Activation temperature, in addition to activation time, is a major factor in determining the BET surface area and yield of carbonized compounds. With an increase in activation temperature, the BET surface area is observed to improve. This is because the release of volatile materials causes the development of new pores and the broadening of existing pores as the temperature rises. Since a large amount of volatile matter is released when the activation temperature is raised, the yield of activated carbon is also reduced.

2.5 DESIGN OF EXPERIMENT

Design of experiment refers to the process of planning, developing, and analyzing an experiment in order to draw reliable and objective results efficiently and decisively. Simple and powerful statistical approaches must be integrated into the experimental

design methodology in order to generate statistically acceptable results from the experiment (del Vecchio, 1997). Any industrially constructed experiment's success is determined by careful planning, suitable design selection, statistical data analysis, and collaborative abilities.

It is regarded as a subset of applied statistics concerned with the design, execution, analysis, and interpretation of controlled experiments in order to determine the factors that influence the value of a parameter or combination of parameters. A design of experiment is a series of tests that involves changing the input variables of a system or a process and measuring the effect on response variables. Design of experiment finds application in both computer simulations and physical processes. It is a very important tool for maximizing the amount of information gained from a study and the amount of data to be collected(Telford, 2007).

The following are some of the goals/ objectives of industry experimentation:

- Enhance yield or efficiency
- Determining the best process settings
- Identifying sources of variation
- Designing new processes and products
- Correlating process variables with product characteristics
- Comparing different processes, machines and materials.
- Reducing development costs.

- Reducing overall cost.(Neubauer, 2008)

In designing of an experiment, the following guidelines can be followed to:

- **Recognition of and Statement of the Problem:** All thoughts regarding the experiment's goals must be developed -everyone's opinion must be gathered -a team approach must be used
- **Choice of Factors, Levels, Response and Range Variables:** It's necessary to rely on engineering judgment or previous test findings.
- **Choice of Experimental Design:** Sample size, replication, run order, randomization, software to utilize, and data collecting form design are all factors to consider while designing an experiment.
- **Performing the Experiment:** it's critical to keep a close eye on the process. In a complicated R&D setting, it's easy to overlook logistical and planning considerations.
- **Statistical Data Analysis:** give objective results and utilize basic graphics whenever possible.
- **Conclusions and Recommendation:** follow up test run and confirmation testing to validate the conclusions from the experiment.

2.5.1 APPLICATION OF DESIGN OF EXPERIMENT

The main applications of design of experiment are listed below;

- Comparative
- Screening / Characterizing factors
- Optimization
- Modeling

COMPARATIVE: Here it functions by determining whether a change in a single aspect has resulted in a change or improvement in the entire process, Selecting between options, having a limited scope and suited for preliminary comparison.

SCREENING/CHARACTERIZING: understanding the process as a whole, in the sense that the designer wants to have a prioritized list of key to minor aspects that affect the process in order to determine which factors are critical.

MODELING: Interested in functionally modeling the process with a well-fitting mathematical function as the output, as well as having reasonable estimates of the coefficients in that function.

OPTIMIZATION: Interested in identifying optimal process factor settings, that is, determining the amount of each factor that improves the process response

The application of design of experiments would lead to;

- Improve the design of your products and processes.

- Increase the development cycle's speed.
- Lower development expenses
- Improve the transition of items from Research & development activities to manufacturing.
- Troubleshoot production issues effectively.
- Achieving product excellence at the lowest total cost possible

2.5.2 FUNDAMENTAL PRINCIPLES OF DESIGN OF EXPERIMENT

The fundamental principles of experimental design are solutions to the challenges in experimentation and they help to improve experiment efficiency. There are three (3) main principles of experimental design;

- Randomization
- Replication
- Blocking

2.5.2.1 Randomization:

Randomization is a method that protects personal bias or preference from distorting the response of a process. Subjects are randomly selected and you guard against either selection bias or accidental bias(Telford, 2007). It is a process used to ensure that each experimental unit has an equal probability of receiving any of the experimental treatments.

Randomization is important because;

- It eliminates prejudice because it must be done through a mechanical process with no subjective human effect on the outcome.
- It eliminates the link between errors.
- It ensures that the results from each of the experimental units are independent.

2.5.2.2 Replication:

Replication is a technique for boosting the precision of an experiment by expanding the sample size. When the noise comes from uncontrollable nuisance variables, replication improves the signal-to-noise ratio. It is the process of applying each factor combination to several experimental units(Telford, 2007).

The major benefit of replication is that it allows the experiment to gain an estimate of the experimental error, which then serves as a fundamental unit of measurement for deciding if observed changes in data are statistically significant. It's a good approach to reduce the impact of uncontrolled variation in an experiment by enhancing precision. Replication is not the same as repeated measurements(Montgomery et al., 2005).

2.5.2.3 Blocking:

Blocking is a technique for improving precision by reducing the impact of recognized bugs. Although both procedures are constantly applied to each batch, blocking is a constraint of total randomization. Since batch-to-batch variability is excluded from the "experimental error," blocking improves precision(Telford, 2007).

Blocking is the process of dividing experimental units into comparable homogeneous groups, each group reflecting a level of the blocking variable. Units in each block are as similar as possible but differ from units in the next block. PH, material kind, moisture level, gradient, age, time of experimentation, and weight location can all be important blocking factors.

2.5.3 TYPE OF DESIGN OF EXPERIMENT

There are various types of experimental designs and they include: factorial design, randomized complete block design (RCBD), central composite design (CCD), Box-Bhenken design (BBD), saturated design and mixture design.

2.5.3.1. Factorial design

Factorial experimentation is a method in which the effects due to each factor and to combinations of factors are estimated. Factorial designs are geometrically constructed and vary all the factors simultaneously and orthogonally. Here, the data are collected at the vertices of a cube in q-dimensions where q is the number of factors being studied(Montgomery et al., 2005). Factorial designs have increased precision over the other types of designs because of their internally built in replications. There are two forms of factorial design and they are:

2.5.3.2. Full factorial design

When all the data are collected form the vertices, it is seen as a full factorial design requiring 2^qruns.Since the total number of combinations increases exponentially with the number of factors studied, fractions of the full factorial design can be constructed.

As the number of factors increases, the fractions become smaller and smaller (1/2,1/4, 1/8, 1/16, …)(Telford, 2007). This is the most common and intuitive strategy of experimental design. Table 2.1 shows an example of 2^3 full factorials experimental design.

Table 2.2: Shows an Example of 2^3 Full Factorials Experimental Design

Experiment Number	Factor level			Response variable	Two and three factor interactions			
	X_1	X_2	X_3		$X_1.X_2$	$X_1.X_3$	$X_2.X_3$	$X_1.X_2.X_3$
1	-1(*l*)	-1(*l*)	-1(*l*)	$y_{l,l,l}$	+1	+1	+1	-1
2	-1(*l*)	-1(*l*)	+1(*h*)	$y_{l,l,h}$	+1	-1	-1	+1
3	-1(*l*)	+1(*h*)	-1(*l*)	$Y_{l,h,l}$	-1	+1	-1	+1
4	-1(*l*)	+1(*h*)	+1(*h*)	$y_{l,h,h}$	-1	-1	+1	-1
5	+1(*h*)	-1(*l*)	-1(*l*)	$y_{h,l,l}$	-1	-1	+1	+1
6	+1(*h*)	-1(*l*)	+1(*h*)	$y_{h,l,h}$	-1	+1	-1	-1
7	+1(*h*)	+1(*h*)	-1(*l*)	$y_{h,h,l}$	+1	-1	-1	-1
8	+1(*h*)	+1(*h*)	+1(*h*)	$y_{h,h,h}$	+1	+1	+1	+1

2.5.3.3. Fractional Factorial Design

When the number of components rises, the full factorial design becomes economically unviable. In that instance, fractional factorial design is utilized (Sethuramiah & Kumar, 2016). Data are collected from a specific subset of all possible vertices and requires require 2p-q runs, with 2-q being the fractional size of the design.

The geometry of the experimental design requires eight runs if there are only three factors present and a one- half fractional factorial experiment (an inscribed tetrahedron) requires four runs (Telford, 2007). Table 2.2 shows and example of 2^{3-1} fractional design

Table 2.3: Shows an Example of 2^{3-1} Factorial Design

Experimental number	Factor level			
	X_1 (A)	X_2 (B)	$X_3(C)=X_1.X_2$	$X_1.X_2.X_3$
1	-1	-1	+1	+1
2	-1	+1	-1	+1
3	+1	-1	-1	+1
4	+1	+1	+1	+1

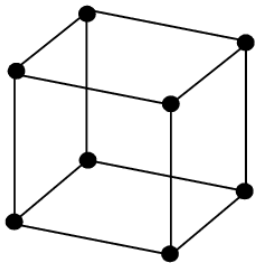

Figure 2.6: full factorial

2.5.3.4. Plackett- Burman designs

A placket-Burman design is a type of screening design that helps to find important factors in an experiment. It was developed by Plackett and Burman in 1946. It screens

out unimportant factors such as noise which means that you avoid collecting large amounts of data on relatively unimportant factors. A placket- Burman design requires to be performed to investigate a maximum of 4n-1 factors at two levels. (Design et al., 2017)

2.5.3.5. Central composite design

A central composite design is a 2^Kfull factorial to which the central point and the star points are added. The star points are the sample points in which all the factors but one is set at the mean level “m”. The value of the remaining factors is given in terms of distance from the central point. The distance of the star points from the central point can be chosen in different ways.

1. If it is set to 1, all the samples are placed on a hypersphere centered in the central point (*central composite circumscribed*, or CCC). This method requires five levels for each factor, namely *ll*, *l*, *m*, *h*, *hh*. This is the most common method used by design of experiment software.

2. If it is set to the value$\frac{\sqrt{K}}{K}$, the parameter remains on the same levels of the 2^K full factorial (*central composite faced*, CCF). The method requires three levels for each factor, namely *l*, *m*, *h*.

3. If it is set to the value$\frac{\sqrt{K}}{K}$, the parameter remains on the same levels of the 2^K full factorial (*central composite faced*, CCF). The method requires three levels for each factor, namely *l*, *m*, *h*,

4. If the distance is set to any other value, whether it is $<\frac{\sqrt{K}}{K}$ (star points inside the design space), <1 (star points inside the hypersphere), or>1 (star points outside the hypersphere), we talk of *central composite scaled*, CCS. The method requires five levels for each factor.

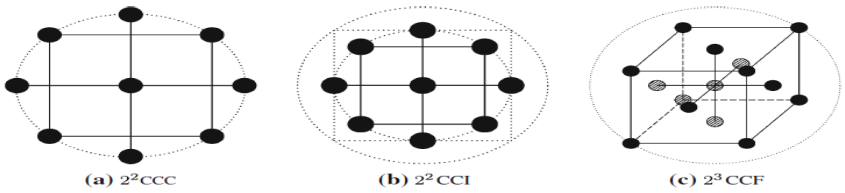

Figure 2.7: Examples of Central composite experimental designs (Cavazzati, 2013)

Table 2.4: Central Composite Design

Factorials	Response	Factors		
		X_1	X_2	X_3
I	*y (l, l, m)*	-1	-1	0
	y (h, l, m)	+1	-1	0
	y (l, h, m)	-1	+1	0
	y (h, h, m)	+1	+1	0

Ii	*y (l, m, l)* *y (h, m, l)* *y (l, m, h)* *y (h, m, h)*	-1 +1 -1 +1	0 0 0 0	-1 -1 +1 +1
Iii	*y (m, l, l)* *y (m, h, l)* *y (m, l, h)* *y (m, h, h)*	0 0 0 0	-1 +1 -1 +1	-1 -1 +1 +1
Iv	*y (m, m, m)*	0	0	0

2.5.3.6. Box-Behnken Design

The Box-Behnken design is an independent quadratic design. It does not contain an embedded factorial or fractional factorial design. They are built combining two-level factorial designs with incomplete block designs in a particular manner. For this design, the treatment combinations are at the midpoints of edges of the sample space and at

the corner.

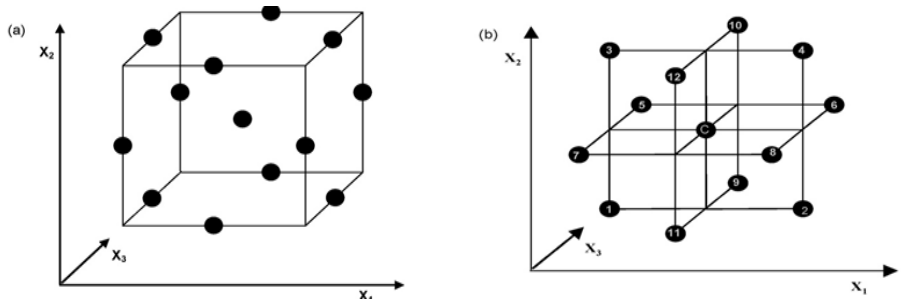

Figure 2.8: box-Behnken Designs

Considering the Box Behnken design with three factors , in this case a 2^2factorial is repeated three times;

I. On the first and the second parameters keeping the third parameter at the mean level (samples are: *llm*, *lhm*, *hlm*, *hhm*).

II. On the first and the third parameters keeping the second parameter at the mean level (samples are: *lml*, *lmh*, *hml*, *hmh*).

III. On the second and the third parameters keeping the first parameter at the mean level (samples: *mll*, *mlh*, *mhl*, *mhh*).

IV. Then the central point (*mmm*), is added

2.5.2.7 Randomized Complete Block Design (RCBD)

The term randomized complete block design (RCBD) refers to the process of determining the total number of experimental units required in the experimentation and then randomly selecting experimental units to be run first or last (Yuangyai & Nembhard,

2010).

2.5.3 RESPONSE SURFACE METHODOLOGY (RSM)

Response surface methodology was first proposed in the early 1930s, but it wasn't fully realized until 1951, due to the efforts of Box and Wilson. Response surface methodology is defined as a set of statistical design and numerical optimization techniques for empirical model construction and model exploitation that are used to optimize processes and product design(Yuangyai & Nembhard, 2010). A response surface is a basic function, such as a linear or quadratic polynomial, that is fitted to the data obtained from the trials, and the approach is known as the response surface method (Box G.E.P. and N.R. Draper, 1987). There are so many works based on the application of RSM in chemical and biochemical process.

Before using the RSM methodology, you must first choose an experimental design that specifies which tests should be conducted in the experimental region under investigation. There are some experimental matrices that can be used for this. When the data set does not contain curvature, experimental designs for first-order models (e.g., factorial designs) can be employed. However, experimental designs for quadratic response surfaces, such as three-level factorial, Box–Behnken, central composite should be used to approximate a response function to experimental data that cannot be explained by linear functions.

RSM assumes that the response of a process is a function of a set of independent variables X_1, X_2, X_3… X_k

$$Y = f(x)\beta + \varepsilon \qquad (2.1)$$

Where $x = (X_1, X_2, X_3 \ldots X_k)$ $f(x)$ is a vector function of p elements that consists of powers and cross products of the powers of $X_1, X_2, X_3, \ldots, X_k$, β is a vector of p unknown constant coefficients called parameters while ε is a random experimental error.
The following are some stages in the application of RSM as an optimization technique:

(1) The selection of independent variables of major effects on the system through screening studies and the delimitation of the experimental region based on the study's objective and the researcher's experience;

(2) The selection of the experimental design and execution of experiments based on the selected experimental matrix;

(3) The mathematical–statistical treatment of the obtained experimental data through the fit of a polynomial function;

(4) The discussion of model's fitness;

(5) Determining the necessity and feasibility of conducting a shift in direction to the optimal zone; and determining the optimum values for each variable under consideration.

CHAPTER THREE

MATERIALS AND METHODOLOGY

3.1 MATERIALS

The chemicals and reagents to be used were obtained in a high analytical grade and are listed as follow;

- Sulphuric acid; 98% pure, produced by Fisons, Loughborough England.
- Lead II chloride; 98% pure, produced by BDH Chemicals ltd, Poole, England.
- EDTA
- Copper sulphate
- Hydrochloric acid (HCL); 37% pure, produced by Guangdong guanghua chemicals factory, china
- Potassium hydroxide (KOH); 97% pure, produced by central drug house ltd New Delhi (India).

Table 3.5: Reagents Used and Their Application

S/N	Reagents Used	Application
1.	Distilled Water	Used for preparation of solutions.
2.	Potassium hydroxide (KOH)	Used as activating agent for

		the char activation.
3.	Sulfuric Acid (H_2SO_4) solution	Used to facilitate neutralization of carbonized char.
4.	Hydrochloric acid (HCl) solution	Used during determination of surface area.
5.	Sodium thiosulfate ($Na_2S_2O_3$) powder	Used as titrant during titration to determine the surface area.
6.	Potassium iodide (KI) powder	Used for the preparation of iodine solution.
7.	Iodine (I_2) crystals	Used for the preparation of iodine solution.
8.	Cassava starch powder	Used for preparation of starch indicator.

Table 3.6: Equipment/Apparatus Used for the Experiment and Their Functions

S/N	Equipment/ Apparatus	Manufacturer and Model Number	Functions
1.	Electric muffle furnace	PEC Medical USA (Model-SX-5-12)	Carbonization of periwinkle shell to char.

2.	Thermostatic Hot Air Drying Oven	DHG-0A Jinotech Instrument Co. China	Drying of adsorbent
3.	Desiccator	S. Pyrex Instruments	Used during cooling processes to prevent moisture gain.
4.	ASTM 250µm sieve	ASTM	Size reduction of the periwinkle shell char for activation
5.	Conical flask	Jinotech instruments	Collection of filtrate during the washing out process.
6.	Filter paper	Whatman	Used to separate washed char residue from the filtrate
7.	Plastic dropper		Used to add minute quantities of sample solutions or reagents.
8.	Plastic funnels		Used during washing out process for filtration
9.	Glass beakers	Jinotech instruments	Used to hold samples for analysis.
10.	Electronic Compact Scale		Used to weigh samples and reagents
11.	Crucibles	ceramics	Used to hold the periwinkle shells during carbonization
12.	Volumetric flask	S.Pryex instruments	Used for making standard

			solutions
13.	Burette	Jinotech instruments	Used to hold titrant during titration process.
14.	Retort stand and clamp	Steel	Used to hold the burette in place during titration.
15.	Measuring cylinder	Jinotech instruments	Measuring volumes of liquids
16.	Cycling vibrator (Orbital shaker)	HY-4A Pec Medical, England	Mixing of adsorbent and effluent
17.	Handheld PH Meter	Juanjuan Digital Digital pH meter Model PH-227H	determination of pH of effluent
18.	Constant Temperature Magnetic Stirrer	MS300 Jinotech Instrument Co., China	stirring adsorbent and effluent mixture with application of heat

3.2 METHODOLOGY

3.2.1 SAMPLE COLLECTION AND PREPARATION

Periwinkle shells were collected as waste in a local market at Uselu, Edo State. The shells were thoroughly washed with warm water to remove soil particles and other undesired materials. The shells were then sun-dried to remove excess water and packed into a polyethylene for further processing in the laboratory.

Figure 3.9: Sorted and Cleaned Periwinkle Shells

3.2.2 CARBONIZATION AND ACTIVATION PROCESS

30.0 grams of periwinkle shells were weighed into 13 crucibles respectively into an electric muffle furnace over the time and temperature stipulated for each run by the experimental design. After heating, the periwinkle shells were left to cool in a desiccator and re-weighed again and noted as w_1 for each run. Each run was grinded and sieved through a 250µm sieve then added to a 250ml beaker and labeled.

In activated carbon preparation, yield is usually defined as final weight of activated carbon produced after activation, washing, and drying, divided by initial weight of raw material; both on a dry basis (Prahas et al., 2008). The percentage yield of activated carbon produced was determined using the equation;

$$\text{yield } \% = \frac{w1}{wo} \times 100 \qquad (3.1)$$

Where, w1 is final weight of the pyrolyzed periwinkle shells).

wo is initial weight of periwinkle shells.

60ml of 0.5M KOH was added to each run and subjected to heat of about 105^0 C in an air drying oven for 2hours. The process of washing out was carried out to neutralize the KOH from the periwinkle shell solution. The process involved adding water and drops of 4% sulfuric acid (H_2SO_4) to the solution and filtering using a filter paper and funnel until neutralization is attained. After neutralization and filtration, each run was dried in the oven at the temp of 110^oC.

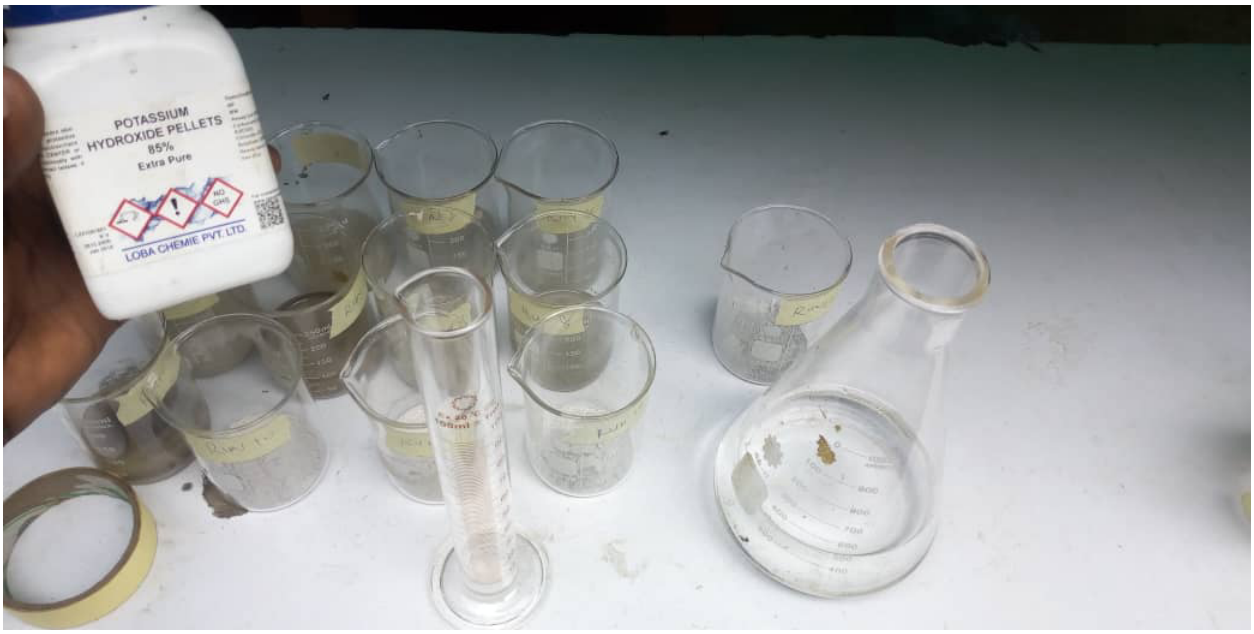

Figure 3.10: Impregnation of Periwinkle Shell Char with KOH

3.2.3 DETERMINATION OF SURFACE AREA BY IODINE NUMBER METHOD

About 10ml of 5% HCl solution was added to 1.0gram of the activated carbon sample and boiled for 60seconds and allowed to cool. Thereafter, 20ml of 2.1M of iodine

solution was added to each of the mixtures and then subjected to intensive checking using an orbital checker for 5minutes. 0.2ml of starch solution was added in drops to 10ml of each HCl-Iodine solution mixture until it turned blue-black.

The HCl-Iodine-starch solution mixture was titrated against 0.1M sodium thiosulfate solution. The titer volumes obtained were recorded for each titration. Blank titration was also carried out without the sample to determine the blank titer volume. To determine the surface area, the iodine number was first calculated using the equation;

$$IN = \frac{Vb-Vs}{m} \times N \times 126.9 \times \frac{Vfb}{Vfs} \qquad (3.2)$$

Where IN represents the iodine number

m is mass of sample

N is normality (0.1N)

Vb is the titre volume of blank

Vs is the titre volume of sample

Vfb = 1

Vfs = 1

The surface area was calculated using the equation;

$$Si = \frac{IN \times 10^{-5}}{mi} \times N \times Wi \qquad (3.3)$$

Where IN is the iodine number

mi = 126.92 g/mol

$N = 6.023 \times 10^{23}\ mol^{-1}$

$Wi = 0.2096 \times 10^{-18}\ m^2$

3.2.4 DETERMINATION OF POROSITY

To determine the porosity, 10ml of each sample was measure into a measuring cylinder and 10ml of water was added to each sample. Each sample was filtered to collect the volume of water that could pass through the sample.

Porosity was calculated for using the equation;

$$\text{porosity} = \frac{Vl}{Vs} \times 100 \qquad (3.4)$$

V_L = volume of liquid that penetrates into the sample

V_S = volume of sample

3.3 DESIGN OF EXPERIMENT

A statistical model for the activated carbon production process was design using the Central Composite Design (CCD) for response surface methodology. Two-independent variables were investigated in this studies for the preparation of AC; they are: x1, activation temperature (°C) and x2, activation time (mins). There are 4 factorial points, 4 axial points and 5 replicates at the center points, indicated by a total of 13 experimental runs for the production process., as calculated by the equation;

$$\text{total number of experiments (N)} = 2^n + 2n + nc = 2^2 + 2\times2 + 5 = 13 \qquad (3.5)$$

Where *n* is the number of factors, nc is the number of center points (six replicates)

The reproducibility of the data and the experimental error were verified using the center points The variables were coded in the (-1, 1) interval, with -1 and +1 representing the

low and high levels, respectively. The axial points are usually located at (±α, 0, 0), (0, ±α, 0), and (0, 0, ±α), where α is the fixed at 1.414. The coded and actual values for the central composite design are shown in table 3.3Table 3.7: Coded and Actual values for the factors of Central Composite Design

Independent Variables	Symbols	Coded and Actual Level				
		-α	-1	0	+1	+α
Activation Temperature (^{o}C)	X1	300	358.58	500	641.42	700
Activation Time (mins)	X2	30	51.97	105	158.03	180

The three responses are activated carbon yield (Y1), surface area (Y2) and porosity (Y3). Each response was used to develop an empirical model which correlated the response to the variables using a second- degree polynomial equation as follow (M. A. Ahmad et al., 2017):

$$Y = bo + \sum_{i=1}^{n} bixi + \left(\sum_{i=1}^{n} biixi\right)^{2} + \sum_{i=1}^{n-1}\sum_{j=1+i}^{n} bijxixj \qquad (3.6)$$

where Y stands for the predicted response,

bo = constant coefficient,

bi = linear coefficients,

bij = interaction coefficients,

bii = quadratic coefficients and

xi and xj stand for coded values of the activated carbon production variables.

The influence of a single factor is represented by the coefficient with one factor, but the interaction of two factors and quadratic effects are represented by the coefficient with two factors and those with second-order terms. The feature of desirability was applied using Design Expert software version 11.1.2.0 to reach a compromise between the results (STAT-EASE Inc., Minneapolis, USA). The coefficient of determination and analysis of variance (ANOVA) were used to evaluate the suitability of the derived model for predicting yield, surface area, and porosity, as well as the significance levels of the linear, interaction, and quadratic factors (Dargahi et al., 2021).

CHAPTER FOUR

RESULTS AND DISCUSSION

4.1 PROPERTIES OF PERIWINKLE SHELLS

The physical properties obtained results of the periwinkle shell-based activated carbons are listed in Table 4.1. The activated periwinkle adsorption efficiency shells is directly related to the total surface area of the carbon (Awokoya et al., 2016). Larger the surface area resulted in higher adsorption efficiency of the carbon, which is an important attribute when considering the selection of adsorbents in the separation process. From the data shown on total surface area in Table 4.1, the periwinkle shell-based activated carbon manufactured in the laboratory had a large total surface area of about 1038 m^2/g. The ash content is a measure of minerals impurities in carbons obtained primarily from carbon precursors. Periwinkle shell-based carbon contained only 0.1 percent ash (Olafadehan et al., 2012).

Table 4.1: Characteristics of Prepared Periwinkle Shell Activated Carbon (PSAC)

Property	Value
Ash Content	97.31%
Specific gravity	1.51
Porosity	75.61%
Particle size	<250μm
pH	7.34

4.2 FOURIER TRANSFORM INFRARED (FTIR) SPECTRA:

Oxygen containing surface functional groups plays important role in influencing the surface properties and adsorption behavior of activated carbons (Dawood & Sen, 2014). These groups can be formed during activation process or can be introduced by oxidation after preparation of activated carbon. The FTIR spectra obtained for the prepared adsorbent is given in Figure 4.1. The sample showed three major absorption bands in the region 1600 – 1400 cm^{-1}. The strong band around 1435 cm^{-1} refers to the stretching vibrations of Carbonate ion (CO_3^{-2}) bonds which is often found in activated carbons. Similarly, the weak peak seen at 3395.60477 cm^{-1} has been assigned to stretching vibrations of Aliphatic primary amine (N – H) bonds. The summary of the results is as presented in Table 4.2.

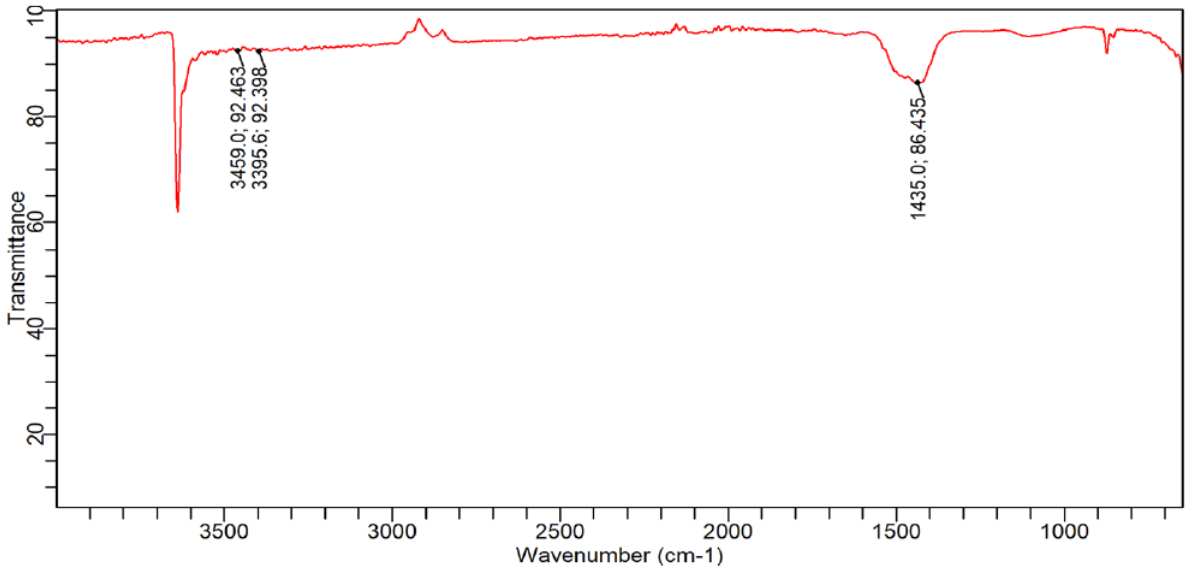

Figure 4.1: FTIR Spectrum of Analysis of Adsorbent

Table 4.2: Result of Spectrum peaks of PSAC.

Peak Number	Wavenumber (cm^{-1})	Intensity	Functional Group	Comment
1	1435.02507	86.43476	Carbonate ion (co_3^{-2})	Strong stretched
2	3395.60477	92.39848	Aliphatic primary amine (N – H)	Weak stretched
3	3458.96951	92.46313	Heterocyclic amine (N – H)	Weak stretched

4.3 MODELING AND ANALYSIS USING RSM

Experimental design for preparing ACs from periwinkle shells (PS) was investigated, using response surface methodology (RSM) to design the experimental work. The two variables investigated were activation temperature (x1) and activation time (x2)) with three responses, including Yield, Y1 (%), surface area, Y2 (m^2/g) and porosity, Y3 (%). These variables were selected based on previous related studies in the literature.

4.3.1 DETERMINATION OF APPROPRIATE MODELS

Design Expert Software was used to analyze the experimental data. Investigation was carried out on linear interaction, two factor interaction and quadratic models to

determine the best statistically significant model and the model that best describes the relationship between the inputs and the response. The models were selected based on the highest order polynomials where the additional terms were significant and the model, not aliased. The model summary statistics of yield, surface area and porosity responses is shown in tables 4.2, 4.3 and 4.4 respectively.

Table 4.3: Model Statistics for Yield (Y1) Response

Source	Std. Dev.	R^2	Adjusted R^2	Predicted R^2	PRESS	
Linear	0.5508	0.9205	0.9045	0.8323	6.40	
2FI	0.3607	0.9693	0.9591	0.9361	2.44	
Quadratic	**0.2568**	**0.9879**	**0.9792**	**0.9379**	**2.37**	**Suggested**
Cubic	0.2899	0.9890	0.9736	0.5644	16.62	Aliased

Table 4.4: Model Statistics for Surface Area Response (Y2)

Source	Std. Dev.	R^2	Adjusted R^2	Predicted R^2	PRESS	
Linear	28.45	0.0116	-0.1861	-0.6364	13404.18	
2FI	29.96	0.0135	-0.3154	-1.2021	18037.97	
Quadratic	**0.4315**	**0.9998**	**0.9997**	**0.9991**	**7.54**	**Suggested**
Cubic	0.3611	0.9999	0.9998	0.9973	22.27	Aliased

Table 4.5: Model Statistics for Porosity Response (Y3)

Source	Std. Dev.	R^2	Adjusted R^2	Predicted R^2	PRESS	
Linear	**0.8016**	**0.9777**	**0.9732**	**0.9544**	**13.12**	**Suggested**
2FI	0.8315	0.9784	0.9711	0.9246	21.67	
Quadratic	0.9317	0.9789	0.9638	0.8685	37.83	
Cubic	0.4880	0.9959	0.9901	0.9455	15.67	Aliased

It shows that quadratic model was generated by RSM as it was statistically significant for yield (Y1) and surface area (Y2) responses. Meanwhile, for porosity (Y3) response, linear model was selected. The generated empirical model by RSM in term of coded factors reflected the interaction and significance of variables towards response. The coefficient with one factor represents the particular factor effect only, whilst the coefficients with two factors and the second-order term represent the interaction of two factors and the quadratic effect, respectively. The final empirical formula models for the responses in terms of coded factors are represented by Equation 4.1;

$$\textbf{Yield}\ (Y1) = 94.76 - 1.32x_1 - 1.63x_2 - 0.6825x_1x_2 + 0.0484x_1^2 - 0.3066x_2^2$$

$$\textbf{Surface}\ \text{Area}(Y2) = 78.48 - 0.986x_1 + 3.30x_2 + 1{,}98x_1x_2 - 32.01x_1^2 - 15.76x_2^2$$

$$\textbf{Porosity}\ (Y3) = 35.49 + 5.88x_1 + 0.7135x_2 \qquad (4.1)$$

Correlation coefficient, R^2 value was very crucial for validation of the model developed.

The R^2 values for equation 4.1 are 0.9879, 0.9998 and 0.9777, respectively. These results indicate 98.79%, 99.98% and 97.77% of the total variation in the PSAC yield, surface area and porosity correlation between the experimental and predicted values, respectively. These high R^2 values show that the predicted responses were near to the experimental values, indicating that the models are adequate for correlating with experiment data. As a result, the R^2 indicates that experimental data are in good agreement. Furthermore, the three models had low standard deviation values of 0.2568, 0.4135, and 0.8016. The complete design matrix for preparing (PSAC) is given in Table 4.5. For the responses, the model coefficient was estimated using multiple regression analysis technique in RSM. It can be seen that the experimental and predicted values obtained were in agreement hence validating the models and results obtained.

Table 4.6: Experimental Design Matrix Coded, Actual Values and Experimental Results for the Responses

Run No	Activation Temperature (°C), X1		Activation Time (mins), X2		Responses					
					Yield (%)		Surface area (m^2/g)		Porosity (%)	
	Coded Values	Actual values	Coded values	Actual values	EXP. Values	PRED. Values	EXP. Values	PRED. Values	EXP. Values	PRED. Values
1	-1	358.579	1	158.033	95.00	94.88	33.14	33.01	30.90	30.32
2	0	500	1.414	180	91.77	91.85	51.74	51.62	37.20	36.50

3	1	641.421	1	158.033	90.97	90.87	34.57	35.00	41.00	42.09
4	1.414	700	0	105	92.83	92.99	13.66	13.06	44.47	43.81
5	0	500	0	105	94.91	94.76	78.13	78.48	35.72	35.49
6	-1.414	300	0	105	96.53	96.73	15.66	15.85	26.10	27.17
7	0	500	0	105	94.97	94.76	78.72	78.48	35.72	35.49
8	0	500	-1.414	30	96.17	96.45	42.59	42.30	33.80	34.48
9	-1	358.579	-1	51.967	97.03	96.77	30.39	30.38	30.00	28.89
10	0	500	0	105	94.50	94.76	78.39	78.48	35.50	35.49
11	0	500	0	105	94.60	94.76	78.81	78.48	34.53	35.49
12	0	500	0	105	94.83	94.76	78.36	78.48	35.42	35.49
13	1	641.421	-1	51.967	95.73	95.49	23.90	24.45	41.00	40.66

4.3.2 ANALYSIS OF VARIANCE (ANOVA)

Through analysis of variance, the models' significance and adequacy were demonstrated (ANOVA). The mean squares were calculated by dividing the total of the squares of each variable source; the model and the error variance were estimated by the degree of freedom. A p-value less than 0.05 shows that the outcome is not random and that the term model has a substantial impact on the answer (M. A. Ahmad et al., 2017). Table 4.5 shows the results of the ANOVA for the quadratic PSAC yield model.

Table 4.7: ANOVA for Quadratic Model of Yield

Source	Sum of Squares	df	Mean Square	F-value	p-value	
Model	37.68	5	7.54	114.26	< 0.0001	significant
X1-Temperature	13.95	1	13.95	211.43	< 0.0001	
X2-Time	21.17	1	21.17	320.88	< 0.0001	
X1X2	1.86	1	1.86	28.25	0.0011	
$X1^2$	0.0163	1	0.0163	0.2468	0.6346	
$X2^2$	0.6540	1	0.6540	9.92	0.0162	
Residual	0.4617	7	0.0660			
Lack of Fit	0.2970	3	0.0990	2.41	0.2079	not significant
Pure Error	0.1647	4	0.0412			
Cor Total	38.15	12				
Std. Dev.	0.2568					
Mean	94.60					
C.V. %	0.2715					
R^2	0.9879					
Adjusted R^2	0.9792					
Predicted R^2	0.9379					

Adequate Precision	33.7789					

From table 4.6, the **Model F-value** of 114.26 and **P-values** less than 0.0500 (0.0001) implied the model were significant. In this case the activation temperature X1, activation time X2, the interaction term of activation temperature and time (X1X2) and the quadratic factor $X2^2$ were significant model terms. Whereas, the quadratic factor $X1^2$ was insignificant to the response. The **Lack of Fit F-value** of 2.41 implied the Lack of Fit was not significant relative to the pure error. Non-significant lack of fit is good. The **Predicted R^2** of 0.9379 was in reasonable agreement with the **Adjusted R^2** of 0.9792; i.e. the difference is less than 0.2. **Adequate Precision** measures the signal to noise ratio. A ratio greater than 4 is desirable. The adequate precision ratio of 33.779 was obtained, thus indicative an adequate signal.

Table 4.8: ANOVA for Quadratic Model of Surface Area

Source	Sum of Squares	df	Mean Square	F-value	p-value	
Model	8190.04	5	1638.01	8799.22	< 0.0001	significant
X1-Activation Temperature	7.78	1	7.78	41.78	0.0003	
X2-Activation Time	86.86	1	86.86	466.59	< 0.0001	
X1X2	15.68	1	15.68	84.24	< 0.0001	
$X1^2$	7129.77	1	7129.77	38300.44	< 0.0001	
$X2^2$	1728.20	1	1728.20	9283.73	< 0.0001	

Residual	1.30	7	0.1862			
Lack of Fit	0.9916	3	0.3305	4.24	0.0982	not significant
Pure Error	0.3115	4	0.0779			
Cor Total	8191.34	12				
Std. Dev.	0.4315					
Mean	49.08					
C.V. %	0.8791					
R^2	0.9998					
Adjusted R^2	0.9997					
Predicted R^2	0.9991					
Adequate Precision	223.1973					

The ANOVA for quadratic model for surface area is shown in Table 4.7. The **Model F-value** of 8799.22 and **model p-value** of < 0.0001 implied the model was significant. The observed P-values less than 0.0500 indicate model terms are significant. In this case X1, X2, X1X2, $X1^2$, $X2^2$ were significant model terms. The **Lack of Fit F-value** of 4.24 was not significant relative to the pure error. The **Predicted R^2** of 0.9991 is in a good agreement with the Adjusted R^2 of 0.9997, of which difference is less than 0.2. **Adequate Precision** measures the signal to noise ratio. A ratio of 223.197 (higher than the desirable ratio of 4) indicated an adequate signal.

Table 4.9: ANOVA for Linear Model of Porosity

Source	Sum of	df	Mean	F-value	p-value	

	Squares		Square			
Model	281.13	2	140.56	218.77	< 0.0001	significant
X1-Activation Temperature	277.06	1	277.06	431.21	< 0.0001	
X2-Activation Time	4.07	1	4.07	6.34	0.0305	
Residual	6.43	10	0.6425			
Lack of Fit	5.46	6	0.9092	3.75	0.1107	not significant
Pure Error	0.9697	4	0.2424			
Cor Total	287.55	12				
Std. Dev.	0.8016					
Mean	35.49					
C.V. %	2.26					
R^2	0.9777					
Adjusted R^2	0.9732					
Predicted R^2	0.9544					
Adequate Precision	43.2268					

The ANOVA for the linear model of PSAC porosity is shown in Table 4.8.The **Model F-value** of 218.77 implied the model was significant. **P-values** less than 0.0500 indicate model terms are significant. In this case X1 and X2 were significant model terms. The **Lack of Fit F-value** of 3.75 implied the Lack of Fit was not significant relative to the pure

error. Non-significant lack of fit is good. The **Predicted R^2** of 0.9544 is in reasonable agreement with the **Adjusted R^2** of 0.9732; i.e. the difference is less than 0.2. **Adequate Precision** measures the signal to noise ratio. A ratio greater than 4 is desirable. A ratio of 43.227 which is greater than the desirable ratio of 4, suggested an adequate signal.

Therefore, it can be concluded that the above models (Equation 4.1) were adequate to predict the PSAC yield, surface area and porosity within the range of variables studied.

4.2.3. PARITY PLOT

The experimental and predicted values shown in Table 4.5 were plotted to analyze the correlation between them as shown in Figure 4.2, 4.3 and 4.4 for yield, surface area and porosity responses respectively. It is observed from the plots that the data points are distributed near the straight line. This further indicates that the models specified for each response could be employed as the significant model for the predicting responses over the independent input variables.

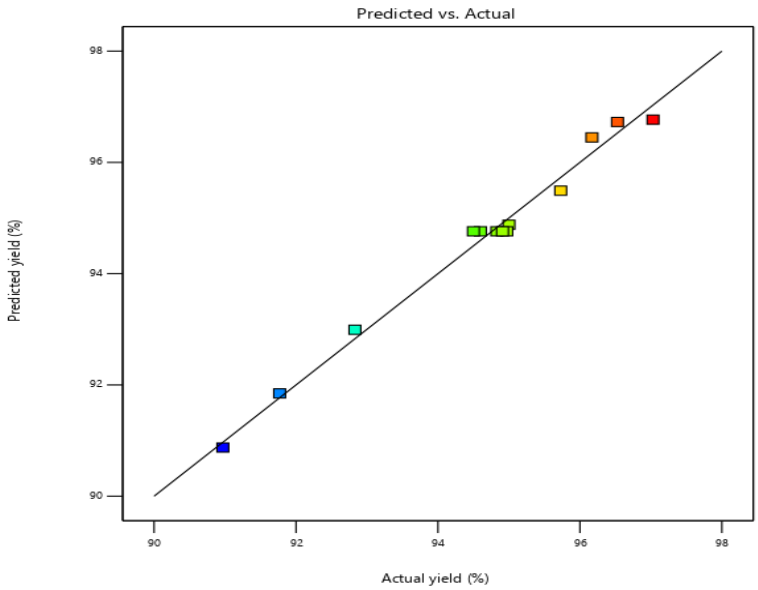

Figure 4.11: Predicted Versus Experimental Values Plot for Yield Response

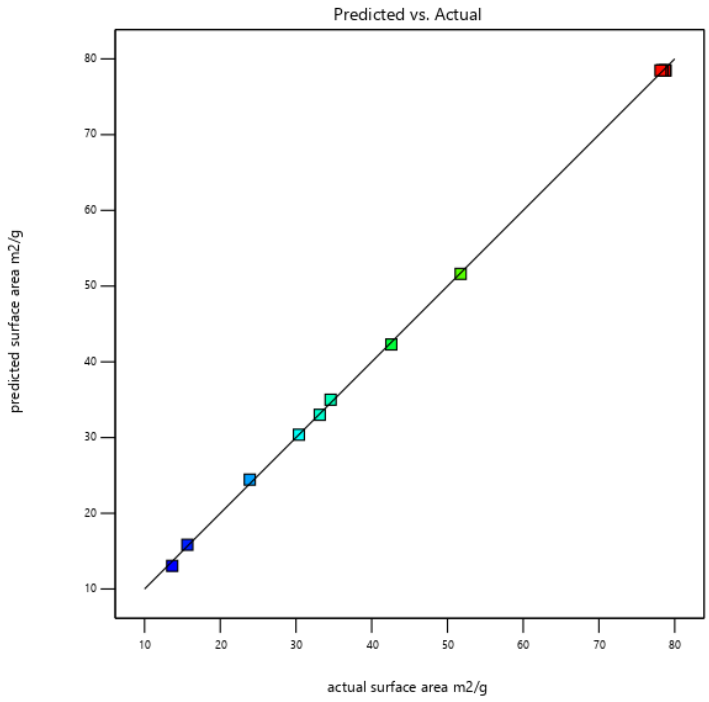

Figure 4.12: Predicted versus actual values plot for Surface Area response

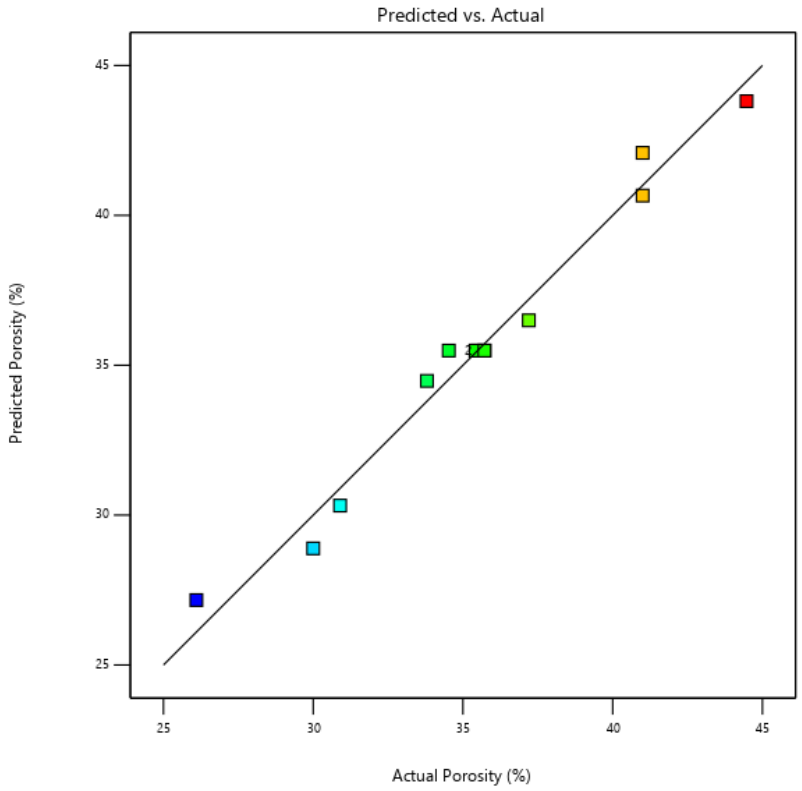

Figure 4.13: Predicted versus Actual values for Porosity response

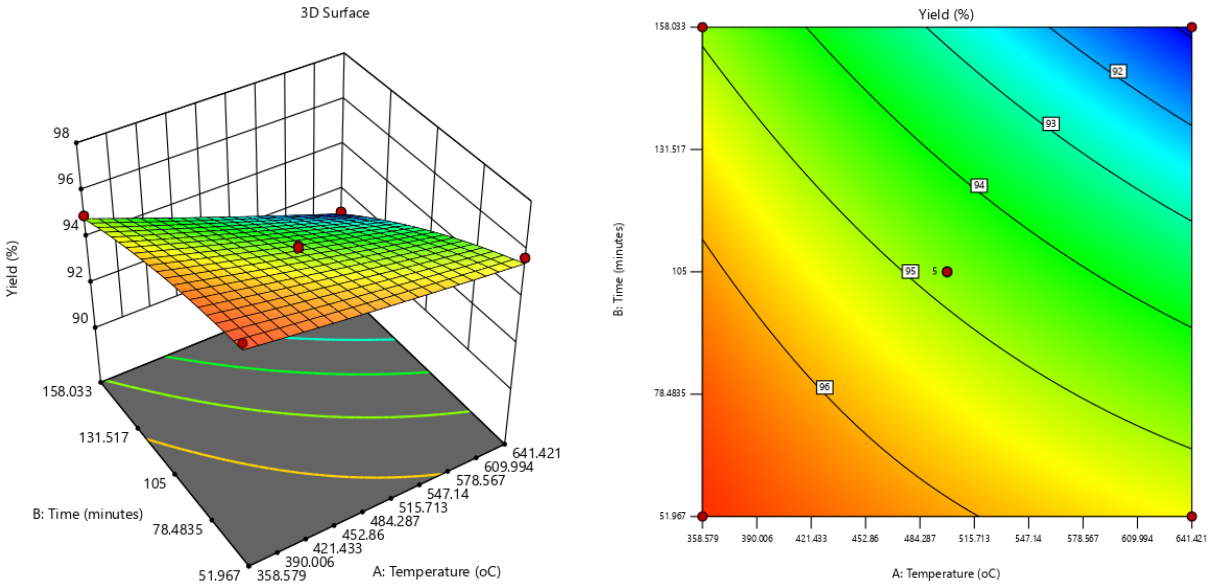

Figure 4.14: 3D Response Surface and Contour Plot for Yield Showing the Influence of

Activation Temperature and Time

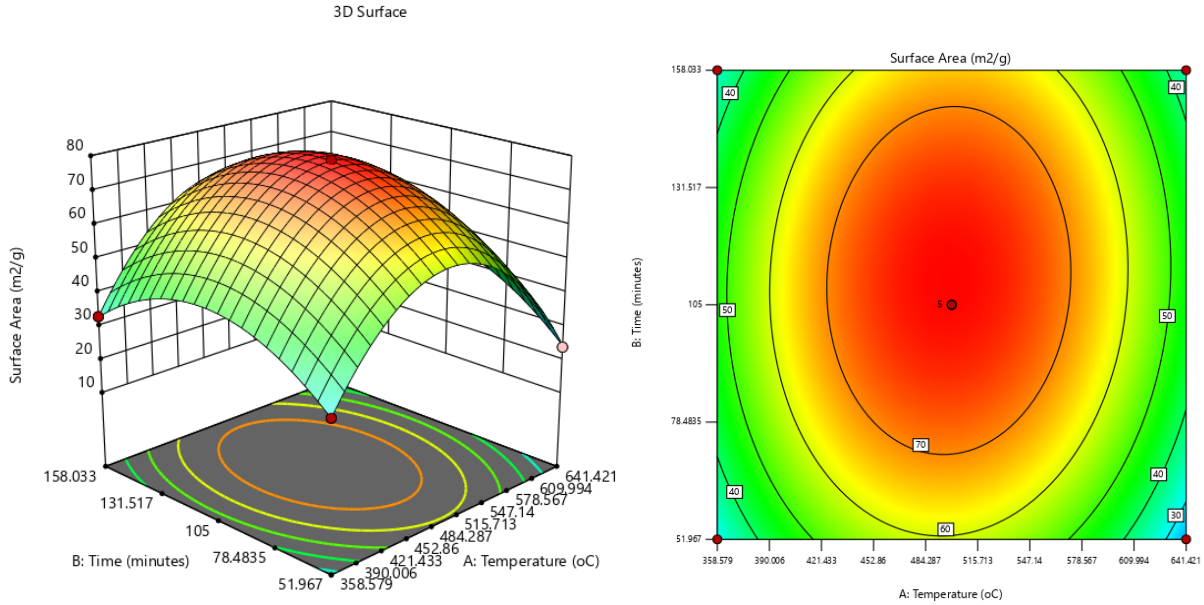

Figure 4.15: 3D Response Surface and Contour Plot for Surface Area to Show the Interaction between Activation Temperature and Time

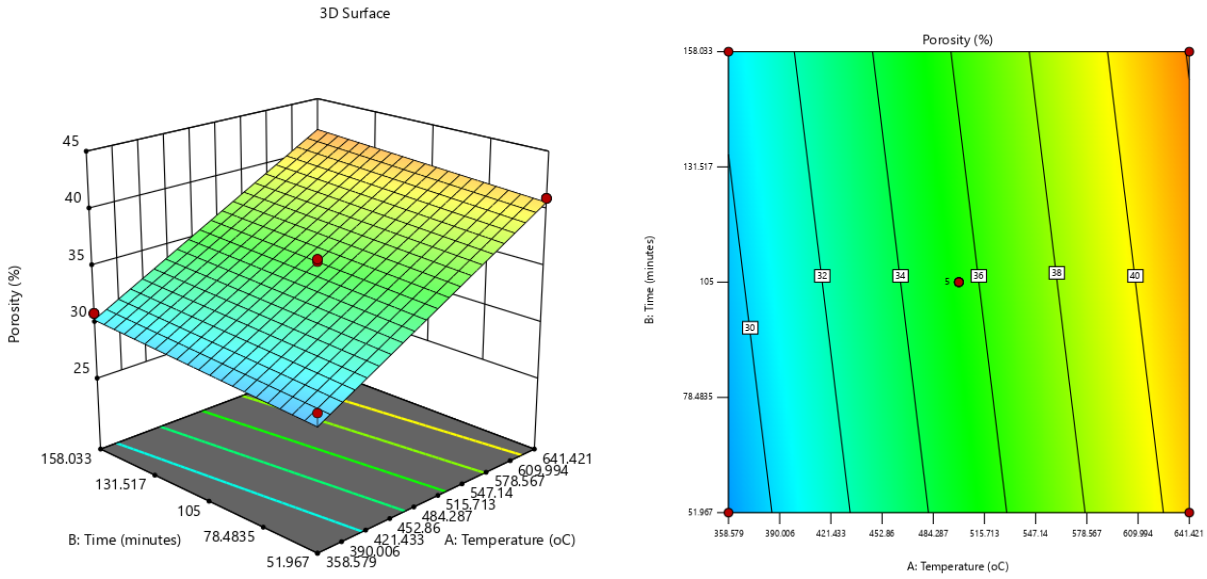

Figure 4.16: 3D Response Surface and Contour Plot Showing the Influence of Activation Temperature and Time on the Porosity

4.4 PSAC Yield

Considering the F-values shown in table 4.6 and the 3-D response surface and contour plot in figure 4.5, it can be implied that both activation temperature and activation time had substantial effect on the yield. However, the activation time has the highest effect on the percentage yield since it gave the highest F-value of 320.88. At 358.579^{o}C and 51.967 minutes, the highest PSAC yield (97.03%) (table 4.4) was achieved. It should be noted that these were the lowest values of the independent variables. This was due to an incomplete elimination process of the volatile matter and tar that took place (M. A. Ahmad et al., 2016) . These volatile matter and tar compounds added more weight to the PSAC, thus higher yield was obtained. Increasing the temperature causes the rate of reactions in C–CO_2 and C–KOH to also increase leading to decrease in carbon yield and increase in carbon “burn-off” by KOH (M. A. Ahmad et al., 2020; Q. S. Liu et al., 2010).

The PSAC yield continued to decrease gradually with increasing activation temperature and time. This result was in accordance with the studies on optimization of preparation conditions for activated carbon from prosopis africana seed hulls using response surface methodology and optimization and batch studies on adsorption of malachite green dye using rambutan seed activated carbon (Rahim & Garba, 2016).

4.5 PSAC Surface Area

From table 4.6, the F-values was indicative that the independent variable; activation temperature and activation time had significant effect on the surface area obtained. Activated time however, had the highest F-value (466.59). The values of surface area achieved ranged from 13.66 – 78.81m^2/g. as presented in table 4.5. It can be seen from the 3D response surface and contour plot that the surface area gradually increased with temperature up to a point and decreased with further temperature increment. When periwinkle shell particles are exposed to high activation temperatures over an extended period of time, the volatile chemicals in the inner half of the particle evaporate. This aids the periwinkle shell particles in acquiring deeper pores, resulting in a larger surface area. With higher activation temperatures, the surface area grows until it reaches a maximum point. Whereas a greater activation temperature is known to provide a large surface area for activated carbon, attempting to create excessively large pores will cause cell wall weakening. The mesopores were generated when many nearby micropores collapsed, reducing the surface area (Y. Liu et al., 2018). As the activating temperature rose over its ideal level, the carbon surface area shrank, resulting in a loss in porosity. The results of this study was in accordance to Influence of different chemical reagents

on the preparation of activated carbons from bituminous coal and optimization of activated carbon preparation from cassava stem using response surface methodology on surface area and yield(Hsu & Teng, 2000; Sulaiman et al., 2018).

4.6 PSAC Porosity

Considering the F-value in table 4.7, it can be implied that both activation temperature and activation time have influenced the porosity achieved. However, the most tangible effect was observed in the activation temperature. It had the highest F- value of 431.21 which greatly outweighs the F-value of 6.34 obtained for the activation time. The highest value of porosity (44.47%) was achieved at 700^{o}C and 105minutes (table 4.5). From figure 4.6, the response surface and contour plot showed an increase of porosity with activation temperature and activation time. The increase in porosity with temperature can be attributed to the release of tars from cross- linked framework generated by the treatment potassium hydroxide (KOH) (Prahas et al., 2008). This result was in accordance with the studies on the production of activated carbon from snail shell waste (*Helix pomatia*) and Influence of different chemical reagents on the preparation of activated carbons from bituminous coal (Gumus & Okpeku, 2015; Hsu & Teng, 2000).

4.7 OPTIMIZATION OF ACTIVATED CARBON PRODUCTION PROCESS

The goal of the experiment was to determine the best production conditions for a high PSAC output, as well as a large surface area and porosity. However, optimizing these three answers under the same condition was difficult due to the different interest zones of variables. Some runs had very high yield matched with low surface area and low porosity and vice versa, hence the need to find the optimum operating conditions to

maximize all responses.

Table 4.10: Optimum Condition for PSAC Production

Temperature	Time	Yield	Surface Area	Porosity	Desirability	
536.375	82.087	95.147	71.525	36.695	0.707	Selected

Table 4.9 shows the optimal condition for activating the carbon that will maximize its responses. Numerical optimization was performed using the Design Expert Software version 11.1.2.0 (STAT-EASE Inc., Minneapolis, USA) to apply the function of desirability to acquire a compromise between these three responses. It was used to optimize the parameters where the target responses were set at maximum values, while the values of variables (activation temperature and activation time) were set in range under study. The optimum conditions the production of activated carbon using periwinkle shell was achieved at activation temperature and activation time of 536.375^{o}C and 82.087mins respectively. These conditions resulted in activated carbon yield of 95.147%`, surface area of 71.525m^{2}/g and porosity of 36.695%.

CHAPTER FIVE

CONCLUSIONS AND RECOMMENDATIONS

5.1 CONCLUSIONS

This study successfully employed response surface methodology (RSM) to examine the influence of the effects of activation temperature and activation time on the percentage yield, surface area and porosity of activated carbon produced from periwinkle shells, PSAC. The models developed for statistical experimental designs and process optimizations were observed. The FTIR analysis was also performed and following conclusions have been drawn;

- Periwinkle shell as a precursor for activated carbon production is very suitable. It is highly carbonaceous and gave high yields that ranged from 90 to 97.03% of activated carbon.

- The quadratic and linear models (p-values<0.0001) developed for statistical experimental designs and process optimization were found to be statistically significant for predicting and understanding the responses as a function of the of process parameters.

- It was found that the optimal activation time and activation temperature is 82.087min and 536.375 °C, respectively gave a predicted response of 95.147% yield, surface area of 71.525m^2/g and 36.695% porosity. Between these two parameters, the activation temperature showed the greatest impact on responses, PSAC yield, surface area and porosity.

- FTIR analysis showed the presence of stretching bands including; the stretching vibrations of Carbonate ion (co_3^{-2}) bonds, aliphatic primary amine (N-H) and heterocyclic amine (N-H).

5.2 RECOMMENDATIONS

Periwinkle shells as activated carbon precursor and agro-wastes has great potentials of replacing commercially made activated carbon (CAC). This is vital because PSACs have the advantage of being more economically and mitigate environmental pollution resulting from periwinkle shells dump. The following are therefore recommended for the purpose of scale up or future researches.

1. More agro-waste products should be investigated to check for their usability for producing value added products so as to further reduce disposals of agro-wastes into the environment.

2. Further studies into the use periwinkle shells for activated carbon production should be carried out to optimize other factors that were not studied in this research and also to improve on the yield, surface area and porosity of the activated carbon.

REFERENCES

Abbas, A. F., & Ahmed, M. J. (2016). Journal of Water Process Engineering Mesoporous activated carbon from date stones (Phoenix dactylifera L .) by one-step microwave assisted K 2 CO 3 pyrolysis. *Journal of Water Process Engineering*, *9*, 201–207. https://doi.org/10.1016/j.jwpe.2016.01.004

Abioye, A. M., & Ani, F. N. (2015). Recent development in the production of activated carbon electrodes from agricultural waste biomass for supercapacitors: A review. *Renewable and Sustainable Energy Reviews*, *52*, 1282–1293. https://doi.org/10.1016/j.rser.2015.07.129

Ahmad, A. A., Din, A. T. M., Yahaya, N. K. E., Khasri, A., & Ahmad, M. A. (2020). Adsorption of basic green 4 onto gasified Glyricidia sepium woodchip based activated carbon: Optimization, characterization, batch and column study. *Arabian Journal of Chemistry*, *13*(8), 6887–6903. https://doi.org/10.1016/j.arabjc.2020.07.002

Ahmad, M. A., Afandi, N. S., Adegoke, K. A., & Bello, O. S. (2016). Optimization and batch studies on adsorption of malachite green dye using rambutan seed activated carbon. *Desalination and Water Treatment*, *57*(45), 21487–21511. https://doi.org/10.1080/19443994.2015.1119744

Ahmad, M. A., Afandi, N. S., & Bello, O. S. (2017). Optimization of process variables by response surface methodology for malachite green dye removal using lime peel activated carbon. *Applied Water Science*, *7*(2), 717–727. https://doi.org/10.1007/s13201-015-0284-0

Ahmad, M. A., Eusoff, M. A., Oladoye, P. O., Adegoke, K. A., & Bello, O. S. (2020). Statistical optimization of Remazol Brilliant Blue R dye adsorption onto activated

carbon prepared from pomegranate fruit peel. *Chemical Data Collections*, *28*, 100426. https://doi.org/10.1016/j.cdc.2020.100426

Arvanitoyannis, I. S., Kassaveti, A., & Ladas, D. (2008). Food Waste Treatment Methodologies. In *Waste Management for the Food Industries*. Elsevier Inc. https://doi.org/10.1016/B978-012373654-3.50009-2

Awokoya, K., Sanusi, R., Oninla, V., & Ajibade, O. (2016). Activated Periwinkle Shells for the Binding and Recognition of Heavy Metal Ions from Aqueous Media. *International Research Journal of Pure and Applied Chemistry*, *13*(4), 1–10. https://doi.org/10.9734/irjpac/2016/31440

Badmus, M. A. O., & Audu, T. O. K. (2009). *Periwinkle Shell : Based Granular Activated Demand (COD) in Industrial Wastewater*. *87*(February), 69–77. https://doi.org/10.1002/cjce.20140

Banerjee, S., De, B., Sinha, P., Cherusseri, J., & Kar, K. K. (2020). Applications of supercapacitors. In *Springer Series in Materials Science* (Vol. 300). https://doi.org/10.1007/978-3-030-43009-2_13

Dargahi, A., Samarghandi, M. R., Shabanloo, A., Mahmoudi, M. M., & Nasab, H. Z. (2021). Statistical modeling of phenolic compounds adsorption onto low-cost adsorbent prepared from aloe vera leaves wastes using CCD-RSM optimization: effect of parameters, isotherm, and kinetic studies. *Biomass Conversion and Biorefinery*. https://doi.org/10.1007/s13399-021-01601-y

Dawood, S., & Sen, T. K. (2014). *Review on Dye Removal from Its Aqueous Solution into Alternative Cost Ef- fective and Non-Conventional Adsorbents*. *1*.

Design, E., Surface, R., & Design, F. (2017). *REVIEW OF EXPERIMENTAL DESIGN IN*

*ANALYTICAL CHEMISTRY T.Sudha * , G.Divya, J.Sujaritha, P. Duraimurugan*. *7*(08).

Eziefula, U. G., Obiechefu, G. C., & Charles, M. E. (2020). Use of periwinkle shell by-products in Portland cement-based materials: An overview. *International Journal of Environment and Waste Management*, *26*(3), 402–422. https://doi.org/10.1504/IJEWM.2020.109165

Faraji, S., & Ani, F. N. (2015). The development supercapacitor from activated carbon by electroless plating - A review. *Renewable and Sustainable Energy Reviews*, *42*, 823–834. https://doi.org/10.1016/j.rser.2014.10.068

Farma, R., Deraman, M., Awitdrus, A., Talib, I. A., Taer, E., Basri, N. H., Manjunatha, J. G., Ishak, M. M., Dollah, B. N. M., & Hashmi, S. A. (2013). Preparation of highly porous binderless activated carbon electrodes from fibres of oil palm empty fruit bunches for application in supercapacitors. *Bioresource Technology*, *132*, 254–261. https://doi.org/10.1016/j.biortech.2013.01.044

Gumus, R. H., & Okpeku, I. (2015). Production of Activated Carbon and Characterization from Snail Shell Waste (<i>Helix</i> <i>pomatia</i>). *Advances in Chemical Engineering and Science*, *05*(01), 51–61. https://doi.org/10.4236/aces.2015.51006

Hsu, L. Y., & Teng, H. (2000). Influence of different chemical reagents on the preparation of activated carbons from bituminous coal. *Fuel Processing Technology*, *64*(1), 155–166. https://doi.org/10.1016/S0378-3820(00)00071-0

Kwiatkowski, M. (2008). Application of fast multivariant identification technique of adsorption systems to analyze influence of production process conditions on obtained microporous structure parameters of carbonaceous adsorbents. *Microporous and Mesoporous Materials*, *115*(3), 314–331.

https://doi.org/10.1016/j.micromeso.2008.02.002

Kwiatkowski, M., & Broniek, E. (2017). An analysis of the porous structure of activated carbons obtained from hazelnut shells by various physical and chemical methods of activation. *Colloids and Surfaces A: Physicochemical and Engineering Aspects*, *529*, 443–453. https://doi.org/10.1016/j.colsurfa.2017.06.028

Kyotani, T. (2003). Porous Carbon. *Carbon Alloys: Novel Concepts to Develop Carbon Science and Technology*, *28*(April), 109–127. https://doi.org/10.1016/B978-008044163-4/50007-3

Liu, Q. S., Zheng, T., Wang, P., & Guo, L. (2010). Preparation and characterization of activated carbon from bamboo by microwave-induced phosphoric acid activation. *Industrial Crops and Products*, *31*(2), 233–238. https://doi.org/10.1016/j.indcrop.2009.10.011

Liu, Y., Zhao, Y., Li, K., Wang, Z., Tian, P., Liu, D., Yang, T., & Wang, J. (2018). Activated carbon derived from chitosan as air cathode catalyst for high performance in microbial fuel cells. *Journal of Power Sources*, *378*(September 2017), 1–9. https://doi.org/10.1016/j.jpowsour.2017.12.019

Mianowski, A., Owczarek, M., & Marecka, A. (2007). Surface area of activated carbon determined by the iodine adsorption number. *Energy Sources, Part A: Recovery, Utilization and Environmental Effects*, *29*(9), 839–850. https://doi.org/10.1080/00908310500430901

Montgomery, D. C., Myers, R. H., & Carter, W. H. (2005). *The Hierarchy Principle in Designed Industrial Experiments*. *September 2003*, 197–201. https://doi.org/10.1002/qre.615

Morris, J. P., Backeljau, T., & Chapelle, G. (2019). Shells from aquaculture: a valuable biomaterial, not a nuisance waste product. *Reviews in Aquaculture*, *11*(1), 42–57. https://doi.org/10.1111/raq.12225

Neubauer, D. V. (2008). Statistical Design of Experiments With Engineering Applications. In *Technometrics* (Vol. 50, Issue 1). https://doi.org/10.1198/tech.2008.s530

Nunes, C. A., & Guerreiro, M. C. (2011). Estimation of surface area and pore volume of activated carbons by methylene blue and iodine numbers. *Quimica Nova*, *34*(3), 472–476. https://doi.org/10.1590/S0100-40422011000300020

Olafadehan, O. A., Jinadu, O. W., Salami, L., & Popoola, O. T. (2012). Treatment Of Brewery Wastewater Effluent Using Activated Carbon. *International Journal of Applied Science and Technology, 2*(1), 165–178.

Olivia, M., Mifshella, A. A., & Darmayanti, L. (2015). Mechanical properties of seashell concrete. *Procedia Engineering*, *125*, 760–764. https://doi.org/10.1016/j.proeng.2015.11.127

Prahas, D., Kartika, Y., Indraswati, N., & Ismadji, S. (2008). Activated carbon from jackfruit peel waste by H3PO4 chemical activation: Pore structure and surface chemistry characterization. *Chemical Engineering Journal*, *140*(1–3), 32–42. https://doi.org/10.1016/j.cej.2007.08.032

Rahim, A. A., & Garba, Z. N. (2016). Optimization of preparation conditions for activated carbon from Prosopis africana seed hulls using response surface methodology. *Desalination and Water Treatment*, *57*(38), 17985–17994. https://doi.org/10.1080/19443994.2015.1086695

Rana, M., Subramani, K., Sathish, M., & Gautam, U. K. (2017). Soya derived heteroatom

doped carbon as a promising platform for oxygen reduction, supercapacitor and CO2 capture. *Carbon*, *114*, 679–689. https://doi.org/10.1016/j.carbon.2016.12.059

Sethuramiah, A., & Kumar, R. (2016). Statistics and Experimental Design in Perspective. In *Modeling of Chemical Wear*. https://doi.org/10.1016/b978-0-12-804533-6.00006-8

Sulaiman, N. S., Hashim, R., Mohamad Amini, M. H., Danish, M., & Sulaiman, O. (2018). Optimization of activated carbon preparation from cassava stem using response surface methodology on surface area and yield. *Journal of Cleaner Production*, *198*, 1422–1430. https://doi.org/10.1016/j.jclepro.2018.07.061

Telford, J. K. (2007). A brief introduction to design of experiments. *Johns Hopkins APL Technical Digest (Applied Physics Laboratory)*, *27*(3), 224–232.

Wang, J., Nie, P., Ding, B., Dong, S., Hao, X., Dou, H., & Zhang, X. (2017). Biomass derived carbon for energy storage devices. *Journal of Materials Chemistry A*, *5*(6), 2411–2428. https://doi.org/10.1039/c6ta08742f

Yahya, M. A., Al-Qodah, Z., & Ngah, C. W. Z. (2015). Agricultural bio-waste materials as potential sustainable precursors used for activated carbon production: A review. *Renewable and Sustainable Energy Reviews*, *46*, 218–235. https://doi.org/10.1016/j.rser.2015.02.051

Yao, Z., Xia, M., Li, H., Chen, T., Ye, Y., & Zheng, H. (2014). Bivalve shell: Not an abundant useless waste but a functional and versatile biomaterial. *Critical Reviews in Environmental Science and Technology*, *44*(22), 2502–2530. https://doi.org/10.1080/10643389.2013.829763

Yuangyai, C., & Nembhard, H. B. (2010). Design of Experiments: A Key to Innovation in

Nanotechnology. In *Emerging Nanotechnologies for Manufacturing* (First Edit). Elsevier Inc. https://doi.org/10.1016/B978-0-8155-1583-8.00008-9

S. M. R. C. P. Ltd, 2018. Activated Carbon - Global Market Outlook (2017-2026). Accessed 14th October, 2021 https://www.jurassiccarbon.com/blogs/news/12186281-the-history-of-activated-carbon

Accessed 15th October,20201 https://en.wikipedia.org/wiki/Activated_carbon#Classification

del Vecchio RJ (1997). Understanding design of experiments: a primer for technologists. Hanser/Gardner Publications Inc., Cincinnati

Box, G. E. P., & Draper, N. R. (1987). *Empirical model-building and response surfaces.* John Wiley & Sons.

F. Derbyshier, M. Jagtoyen, M. Thawaites, in: J.W. Patrick (Ed.), (1997) Porosity in Carbons: Characterization and Applications, Edward Arnold, London, p. 227

APPENDIX

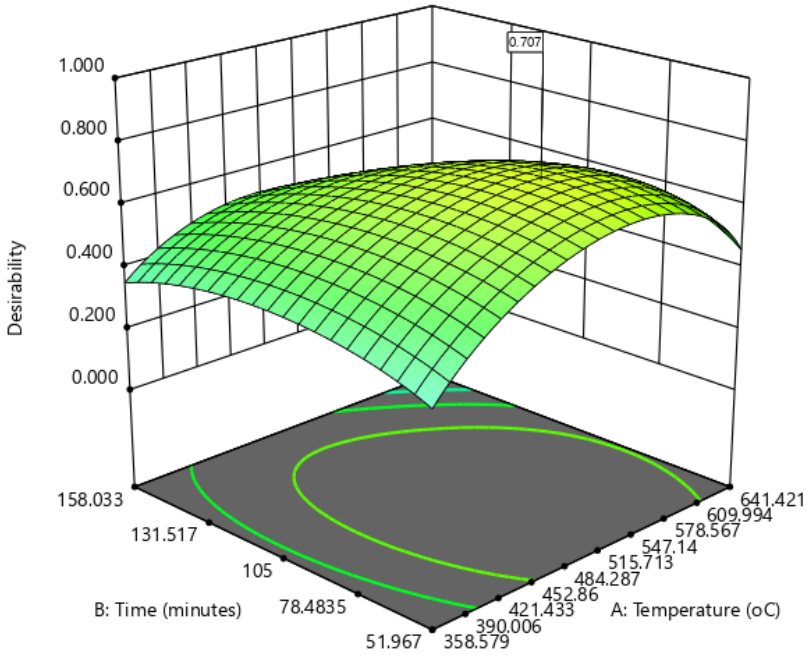

Figure 18: 3D Response Surface plot showing desirability of optimal conditions

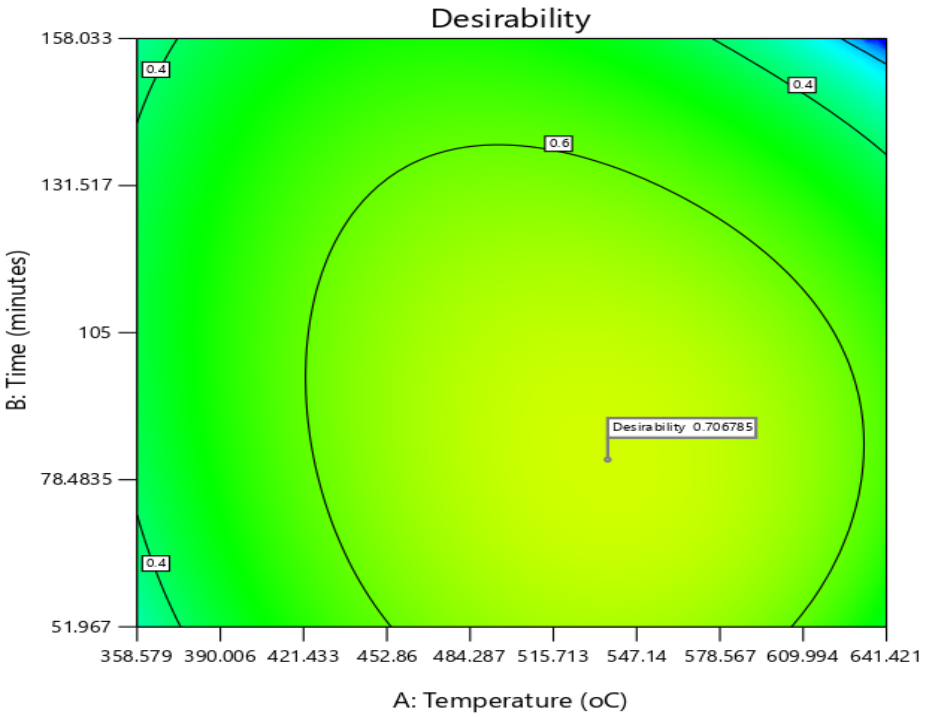

Figure 19: Contour Plot of Desirability of Optimal Conditions

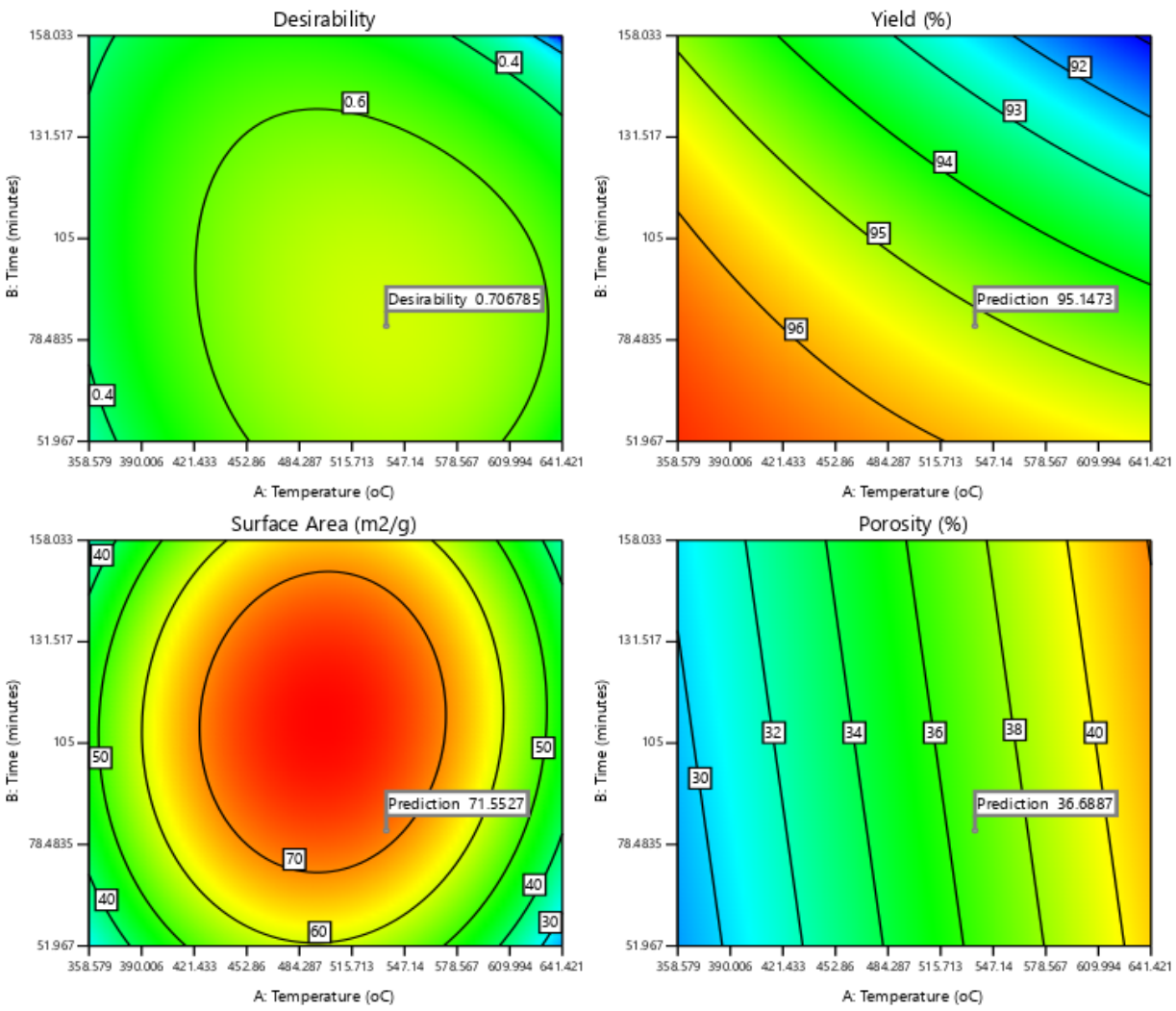

Figure 20: Contour plots showing interaction of activation temperature and activation time for the different responses at optimal conditions